

Towards a holographic dual of large- N_c QCD

Martin Kruczenski,^a David Mateos,^b Robert C. Myers^{b,c} and David J. Winters^{b,d}

^a Department of Physics, Brandeis University
Waltham, MA 02454, USA

^b Perimeter Institute for Theoretical Physics
Waterloo, Ontario N2J 2W9, Canada

^c Department of Physics, University of Waterloo
Waterloo, Ontario N2L 3G1, Canada

^d Department of Physics, McGill University
Montreal, Quebec H3A 2T8, Canada

E-mail: martink@brandeis.edu, dmateos@perimeterinstitute.ca,
rmyers@perimeterinstitute.ca, winters@physics.mcgill.ca

Abstract: We study N_f D6-brane probes in the supergravity background dual to N_c D4-branes compactified on a circle with supersymmetry-breaking boundary conditions. In the limit in which the resulting Kaluza-Klein modes decouple, the gauge theory reduces to non-supersymmetric, four-dimensional QCD with N_c colours and $N_f = N_c$ flavours. As expected, this decoupling is not fully realised within the supergravity/Born-Infeld approximation. For $N_f = 1$ and massless quarks, $m_q = 0$, we exhibit spontaneous chiral symmetry breaking by a quark condensate, $h \neq 0$, and find the associated massless pion' in the spectrum. The latter becomes massive for $m_q > 0$, obeying the Goldstone-Mann-Neunes-Renner relation: $M^2 = m_q h \propto f^2$. In the case $N_f > 1$ we provide a holographic version of the Vafa-Witten theorem, which states that the (N_f) flavour symmetry cannot be spontaneously broken. Further, we find $N_f^2 - 1$ unexpectedly light scalar mesons in the spectrum. We argue that these are not (pseudo-)Goldstone bosons and speculate on the string mechanism responsible for their lightness. We then study the theory at finite temperature and exhibit a phase transition associated with a discontinuity in $h \propto T$. D6/D6 pairs are also briefly discussed.

Keywords: D-branes, Supersymmetry and Duality.

Contents

1. Introduction and summary of results	1
2. Chiral symmetry breaking from D 6-brane embeddings	5
2.1 The D 4-soliton background	5
2.2 D 6-brane embeddings	7
3. Meson spectroscopy from D 6-brane fluctuations ($N_f = 1$)	13
3.1 Analysis of the spectrum	13
3.2 Stability Issues	19
4. The pseudo-Goldstone boson	20
5. Multiple flavours ($N_f > 1$) and a holographic Vafa-Witten theorem	24
6. Finite Temperature Physics	27
7. D 4/D 6/ $\overline{D 6}$ -intersections	34
8. Discussion	37

1. Introduction and summary of results

The AdS_5/CFT_4 correspondence relates string theory on the near-horizon background of N_c D 3-branes to the conformal field theory living on their worldvolume [1]. Inspired by this correspondence, Witten proposed a construction of the holographic dual of four-dimensional, pure $SU(N_c)$ Yang-Mills (YM) theory [2]. One starts with N_c D 4-branes compactified on a circle of radius M_{KK}^{-1} , and further imposes anti-periodic boundary conditions for the worldvolume fermions on this circle. Before compactification, the D 4-brane theory is a five-dimensional, supersymmetric $SU(N_c)$ gauge theory whose field content includes fermions and scalars in the adjoint representation of $SU(N_c)$, in addition to the gauge fields. At energies much below the compactification scale, M_{KK} , the theory is effectively four-dimensional. The anti-periodic boundary conditions break all of the supersymmetries and give a tree-level mass to the fermions, while the scalars also acquire a mass through one-loop effects. Thus at sufficiently low energies the dynamics is that of four-dimensional, massless gluons.

The D 4-brane system above has a dual description in terms of string theory in the near-horizon region of the associated (non-supersymmetric) supergravity background. Unfortunately, as observed in [2], the Kaluza-Klein (KK) modes on the D 4-brane do not decouple

within the supergravity approximation. For example, the mass of the lightest glueball is of the same order as the strong coupling scale. In this sense, there is no energy region, $E \ll M_{KK}$, in which a description in terms of weakly-coupled gluons is appropriate. Nevertheless, the qualitative features of the glueball spectrum agree with lattice calculations [3], and the supergravity description succeeds, for example, to exhibit an area law for Wilson loops [2].

Since most of our phenomenological understanding of low-energy QCD comes from the study of mesons and baryons, it is interesting to construct a holographic dual of a gauge theory whose low-energy degrees of freedom consist not only of gluons but also of fundamental quarks. In the context of AdS/CFT, fundamental matter can be added to the gauge theory by introducing D-brane probes in the dual supergravity background [4, 5, 6]. This has been recently exploited to study mesons holographically in several examples of gauge/gravity duals [7, 8, 9, 10]. The goal of this paper is to study a gauge/gravity dual in which the gauge theory reduces to non-supersymmetric, four-dimensional QCD in the limit in which the KK modes decouple. The construction is as follows.

Consider the D4/D6 system with the branes oriented as described by the following array:

$$\begin{aligned} N_c D4: & 0 1 2 3 4 - - - - \\ N_f D6: & 0 1 2 3 - 5 6 7 - - : \end{aligned} \tag{1.1}$$

Note that the D4- and the D6-branes may be separated from each other along the 89-directions. This system is T-dual to the D3/D5 intersection, and in the decoupling limit for the D4-branes [11] provides a non-conformal version of the AdS/dCFT correspondence [5, 12]. On the gauge theory side one has a supersymmetric, four-dimensional $SU(N_c)$ gauge theory coupled to a four-dimensional defect. The entire system is invariant under eight supercharges, that is, $N = 2$ supersymmetry in four-dimensional language. The degrees of freedom localized on the defect are N_f hypermultiplets in the fundamental representation of $SU(N_c)$, which arise from the open strings connecting the D4- and the D6-branes. Each hypermultiplet consists of two Weyl fermions of opposite chiralities, $_{L,R}$, and two complex scalars.

As discussed above, identifying the 4-direction with period $2\pi M_{KK}$, and with anti-periodic boundary conditions for the D4-brane fermions, breaks all of the supersymmetries and renders the theory effectively four-dimensional at energies $E \ll M_{KK}$. Further, the adjoint fermions and scalars become massive. Now, the bare mass of each hypermultiplet, m_q , is proportional to the distance between the corresponding D6-brane and the D4-branes. Even if these bare masses are zero, we expect loop effects to induce a mass for the scalars in the fundamental representation. Generation of a mass for the fundamental fermions is, however, forbidden by a chiral, $U(1)_A$ symmetry that rotates $_{L,R}$ with opposite phases.¹ Therefore, at low energies, we expect to be left with a four-dimensional $SU(N_c)$ gauge theory coupled to N_f flavours of fundamental quark.

¹This symmetry would be broken by instanton effects but these vanish in the large- N_c limit in which supergravity is valid.

In the dualstring theory description, the D 4-branes are again replaced by their supergravity background. In the so-called ‘probe limit’, $N_f \ll N_c$, the backreaction of the D 6-branes on this background is negligible and hence they can be treated as probes. The D 6-brane worldvolume fields are dual to gauge-invariant field theory operators constructed with at least two hypermultiplet fields, that is, meson-like operators; of particular importance here will be the quark bilinear operator, $\bar{q}_L^i q_L^i + \bar{q}_R^i q_R^i$, where $i = 1, \dots, N_f$ and $i = 1, \dots, N_f$ is the flavour index. In the string description the $U(1)_A$ symmetry is nothing but the rotation symmetry in the $(8,9)$ -plane. In addition to acting on the fermions as explained above, this symmetry also acts on the adjoint scalar $X = X^8 + iX^9$ by a phase rotation.

Having presented the general construction, we now summarise our main results.

We begin in section 2 by considering the case of a single D 6-brane. For $m_q = 0$, we expect the chiral $U(1)_A$ symmetry to be spontaneously broken by a chiral condensate, $h \neq 0$, and there to be an associated massless Goldstone boson in the spectrum, as in QCD with one massless flavour. In QCD, this is the π^0 (which becomes massless in the large- N_c limit), but, in an abuse of language, we will refer to it as a ‘pion’. We are indeed able to show that the string description provides a holographic realisation of this physics, by showing that the $U(1)_A$ symmetry is spontaneously broken by the brane embedding, as in [9]. Moreover, we numerically determine the chiral condensate for an arbitrary quark mass. We find $h \propto (m_q = 0) \neq 0$, as expected, and $h \propto (m_q) / 1 = m_q$ for $m_q \neq 0$, again in agreement with field theory expectations (which we briefly review).

In sections 3 and 4 we study the meson spectrum. We first show analytically, in section 3, that at $m_q = 0$ there is exactly one normalizable, massless (in the four-dimensional sense) fluctuation of the D 6-brane. This open-string mode corresponds precisely to the Goldstone mode of the D 6-brane embedding. If $m_q > 0$, this pion becomes a pseudo-Goldstone boson. We are able to show, analytically, that its squared mass scales linearly with the quark mass, M^2 / m_q , in the limits of small (section 4) and large (section 3) quark mass. With numerical calculations we then confirm that, in fact, such a linear relation holds for all quark masses. For small m_q this linear relation is in perfect agreement with the Gell-Mann-Oakes-Renner (G M O R) relation [13],

$$M^2 = \frac{m_q h \propto}{f^2}; \quad (1.2)$$

which gives the first term in the expansion of the pion mass around $m_q = 0$. In section 4, we compute the chiral condensate and the pion decay constant analytically (at $m_q = 0$), and with these results we are able to verify that, for small quark mass, the mass of our pion precisely satisfies the G M O R relation. In the opposite limit, $m_q \neq 0$, we show in section 3 that

$$M^2 = a \frac{m_q M_{KK}}{g_{YM}^2 N_c}; \quad (1.3)$$

where a is a pure number; for the lightest mesons, we find $a = 20$.

The remaining mesons (D 6-brane excitations) are studied in section 3. Form q . M_{susy} , where

$$M_{susy} = g_{YM}^2 N_c M_{KK}; \quad (1.4)$$

they all have masses of order the compactification scale, M_{KK} , and so the (pseudo-)Goldstone boson dominates the infrared physics in the regime of small q . Of course, this result signals the lack of decoupling between the KK and the QCD scales within the supergravity/Born-Infeld approximation, as expected. Form q & M_{susy} supersymmetry is approximately restored, the spectrum exhibits the corresponding degeneracy, and all meson masses obey a formula like (1.3) with appropriate values of a . The fact that supersymmetry is restored at $m_q = M_{susy}$ suggests that the effective mass of some of the microscopic degrees of freedom must be at least of order M_{susy} . We close section 3 with an examination of certain stability issues for the D 6-brane embeddings.

In section 5, for the case of multiple flavours, $N_f > 1$, we provide a holographic version of the Vafa-Witten theorem [4], which states that the $U(N_f)$ flavour symmetry cannot be spontaneously broken if $m_q > 0$. In the holographic description this is realised by the fact that the N_f D 6-branes must be coincident in order to minimise their energy.

In section 6, we examine the theory at finite temperature. If $m_q > M_{susy}$, the theory exhibits two phase transitions: the first one is the well-known confinement/deconfinement transition at $T = T_{deconf} = M_{KK}$ [2], and the second one is a phase transition at

$$T = T_{fund} \quad \frac{m_q M_{KK}}{g_{YM}^2 N_c} > T_{deconf}; \quad (1.5)$$

characterised by a discontinuity in the chiral condensate, $h_i(T)$, and in the specific heat. If $m_q < M_{susy}$ the second transition does not occur as a separate phase transition.

In section 7 we discuss six-brane embeddings that, from the brane-construction viewpoint, correspond not to D 4/D 6 intersections but to intersections of D 4-branes with D 6/ $\overline{D 6}$ pairs. From the gauge theory viewpoint these configurations correspond to having a defect/anti-defect pair.

We close with a brief discussion of our results in section 8. In particular, one result of the analysis of the $N_f > 1$ case in section 5 is the existence of N_f^2 massless scalar mesons in the gauge theory spectrum if $m_q = 0$. (We expect the inclusion of sub-leading effects in the $1=N_c$ expansion to generate small masses for these particles.) Although it is tempting to interpret these particles as Goldstone bosons of a putative, spontaneously-broken $U(N_f)_A$ chiral symmetry, we argue that this interpretation cannot be correct: even at large N_c , only one of them is a true Goldstone boson. Thus we are unable to find any obvious reasons, from the viewpoint of the four- or ve -dimensional gauge theory, for these scalars to be light. We speculate that, from the string viewpoint, ten-dimensional $U(N_f)$ gauge invariance (as opposed to just seven-dimensional gauge invariance on the D 6-branes) is responsible for their lightness.

2. Chiral symmetry breaking from D 6-brane embeddings

In this section we will show how the spontaneous breaking of the $U(1)_A$ chiral symmetry expected from the field theory side is realized in the string description.

2.1 The D 4-soliton background

The type IIA supergravity background dual to N_c D 4-branes compactified on a circle with anti-periodic boundary conditions for the fermions takes the form

$$ds^2 = \frac{U}{R}^{3=2} dx^0 dx^0 + f(U) d^2 + \frac{R}{U}^{3=2} \frac{dU^2}{f(U)} + R^{3=2} U^{1=2} d^2_4; \quad (2.1)$$

$$e = g_s \frac{U}{R}^{3=4}; \quad F_4 = \frac{N_c}{V_4} d^4; \quad f(U) = 1 - \frac{U_{KK}^3}{U^3}; \quad (2.2)$$

The coordinates $x^0 = fx^0, \dots, x^3$ parametrize the four non-compact directions along the D 4-branes, as in (1.1), whereas d^2_4 parametrizes the circular 4-direction on which the branes are compactified. d^2_4 and d^4 are the SO(5)-invariant line element and volume form on a unit four-sphere, respectively, and $V_4 = 8\pi^2/3$ is its volume. U has dimensions of length and may be thought of as a radial coordinate in the 56789-directions transverse to the D 4-branes. To avoid a conical singularity at $U = U_{KK}$, U must be identified with period

$$= \frac{4}{3} \frac{R^{3=2}}{U_{KK}^{1=2}}; \quad (2.3)$$

Following the nomenclature of [15], we refer to this solution as the D 4-soliton.

This supergravity solution above is regular everywhere and is completely specified by the string coupling constant, g_s , the Ramond-Ramond flux quantum (i.e., the number of D 4-branes), N_c , and the constant U_{KK} . The remaining parameter, R , is given in terms of these quantities and the string length, ℓ_s , by

$$R^3 = g_s N_c \ell_s^3; \quad (2.4)$$

If U_{KK} is set to zero, the solution (2.1, 2.2) reduces to the extremal, 1/2-supersymmetric D 4-brane solution. Hence we may say that U_{KK} characterises the deviation of the D 4-soliton from extremality.

The $SU(N_c)$ field theory dual to (2.1, 2.2) is defined by the compactification scale, M_{KK} , below which the theory is effectively four-dimensional, and the four-dimensional coupling constant at the compactification scale, g_{YM} . These are related to the string parameters by

$$M_{KK} = \frac{3U_{KK}^{1=2}}{2R^{3=2}} = \frac{3}{2} \frac{U_{KK}^{1=2}}{(g_s N_c)^{1=2} \ell_s^{3=2}}; \quad g_{YM}^2 = \frac{3}{2} - \frac{g_s U_{KK}^{1=2}}{N_c \ell_s^3}; \quad (2.5)$$

The first equation follows from the fact that M_{KK} is directly identified with the compact direction in the gauge theory, so $M_{KK} = 2 = \ell_s$. The second equation follows from the fact that

$g_5^2 = (2\pi)^2 g_s^2$ and the relation between the four- and ve-dimensional coupling constants, $g_{YM}^2 = g_5^2 = \dots$, which can be seen by expanding the Born-Infeld action of the D 4-brane and adopting the standard normalization for the gauge field kinetic term, $F^2 = 4g_5^2$.

It is useful to invert these relations to express the string parameters in terms of the gauge theory ones:

$$R^3 = \frac{1}{2} \frac{g_{YM}^2 N_c}{M_{KK}} \sqrt{s} ; \quad g_s = \frac{1}{2} \frac{g_{YM}^2}{M_{KK}} \sqrt{s} ; \quad U_{KK} = \frac{2}{9} g_{YM}^2 N_c M_{KK} \sqrt{s}^2 ; \quad (2.6)$$

The string length will cancel in any calculation of a physical quantity in the field theory. For example, the QCD string tension is²

$$= \frac{1}{2} \frac{p}{\sqrt{s}} \frac{G_{tt} G_{xx}}{U = U_{KK}} = \frac{1}{2} \frac{\sqrt{s}}{R} \frac{U_{KK}}{R}^{3/2} = \frac{2}{27} g_{YM}^2 N_c M_{KK}^2 ; \quad (2.7)$$

Now we may ask in what situation the D 4-soliton provides a reliable background in which one can study the dual field theory using only supergravity. First, we must require that the curvature is everywhere small compared to the fundamental string tension. This ensures that higher derivative string corrections to the low energy equations of motion are negligible. The maximum curvature in the geometry given by (2.1) occurs at precisely $U = U_{KK}$, where the curvatures are of the order $(U_{KK} R^3)^{1/2}$. Hence we require

$$\frac{U_{KK}^{1/2} R^{3/2}}{\sqrt{s}} , \quad g_{YM}^2 N_c \ll 1 ; \quad (2.8)$$

where we have applied the results in eq. (2.6). Therefore the restriction to small curvatures corresponds to a large 't Hooft coupling in the effective four-dimensional gauge theory, precisely as in the conventional AdS/CFT correspondence [1]. Further, to suppress string loop effects, we must also require that the local string coupling, e , be small. Using eqs. (2.2) and (2.6) we see that, for finite values of the gauge theory parameters, the inequality $e \ll 1$ can only be satisfied up to some critical radius

$$U_{crit} , \quad \frac{N_c^{1/3} M_{KK} \sqrt{s}}{g_{YM}^2} : \quad (2.9)$$

Beyond this radius, the M-theory circle opens up to reveal an AdS₇ × S⁴ background (with identifications). Similarly, at the corresponding high energy scales, the ve-dimensional Yang-Mills theory reveals a UV completion in terms of the (2,0) theory compactified on a circle. In the present context, we naturally demand that $U_{crit} \ll U_{KK}$, which, using (2.9) and (2.6), reduces to

$$g_{YM}^4 \frac{1}{g_{YM}^2 N_c} \ll 1 ; \quad (2.10)$$

where the second inequality follows from eq. (2.8). Eqs. (2.8) and (2.10) imply that the supergravity analysis in the D 4-soliton background is reliable in precisely the strong-coupling regime of the 't Hooft limit of the four-dimensional gauge theory: $g_{YM} \gg 0, N_c \gg 1, g_{YM}^2 N_c$ fixed and large.

²This is the tension of a string lying at $U = U_{KK}$ and extending along x . It can also be computed by projecting such a string onto the boundary and integrating $h F^2$ across a transverse section of the string [17].

2.2 D 6-brane embeddings

We are now ready to study the embedding of a D 6-brane probe in the D 4-soliton geometry. Asymptotically (as $U \rightarrow 1$), the D 6-brane is embedded as described by the array (1.1). The analysis is greatly simplified by introducing isotropic coordinates in the 56789-directions. Towards this end, we first define a new radial coordinate, ρ , related to U by

$$U(\rho) = \frac{U_{KK}^{3=2}}{4^{3=2}} \rho^{2=3}; \quad (2.11)$$

and then we coordinates $z = (z^5; \dots; z^9)$ such that $\rho = \sqrt{z^5}$ and $dz = d\rho + \rho^2 d\theta^2$. In terms of these coordinates the metric (2.1) becomes

$$ds^2 = \frac{U}{R} \left(dx^2 + f(U) d\rho^2 + K(\rho) d\theta^2 \right); \quad (2.12)$$

where

$$K(\rho) = \frac{R^{3=2} U^{1=2}}{2}; \quad (2.13)$$

Here U is now thought of as a function of ρ . Finally, to exploit the symmetries of the D 6-brane embedding we seek, we introduce spherical coordinates $\theta^1, \dots, \theta^7$ for the $z^{5,6,7}$ -space and polar coordinates r, θ^8, θ^9 for the $z^{8,9}$ -space. The final form of the D 4-brane metric is then

$$ds^2 = \frac{U}{R} \left(dx^2 + f(U) d\rho^2 + K(\rho) d\theta^2 + \rho^2 d\theta^2 + dr^2 + r^2 d\theta^2 \right); \quad (2.14)$$

where $\theta^2 = \theta^2 + r^2$.

In these coordinates the D 6-brane embedding takes a particularly simple form. We use x^0, \dots, x^7 (or $x^a, a = 0, \dots, 6$, collectively) as worldvolume coordinates. The D 6-brane's position in the 89-plane is specified as $r = r(\theta^8, \theta^9)$, $\rho = \rho_0$, where ρ_0 is a constant. Note that ρ is the only variable on which r is allowed to depend, by translational and rotational symmetry in the 0123- and 567-directions, respectively. We also set $\rho = \text{constant}$ in the following, which corresponds to a single D 6-brane localized in the circle direction. We will study configurations in which this condition is relaxed in section 7.

With this ansatz for the embedding, the induced metric on the D 6-brane, g_{ab} , takes the form

$$ds^2(g) = \frac{U}{R} \left(dx^2 + K(\rho) \left(1 + \frac{r^2}{\rho^2} \right) d\theta^2 + \rho^2 d\theta^2 \right); \quad (2.15)$$

where $r = \rho \theta$. The D 6-brane action becomes

$$S_{D6} = \frac{1}{(2\pi)^6 \sqrt{s}} \int d^7x \sqrt{-g} = \frac{1}{T_6} \int d^7\theta \sqrt{h} \left(1 + \frac{U_{KK}^{3=2}}{4^{3=2}} \rho^2 \right)^{1/2} \sqrt{1 + \frac{r^2}{\rho^2}}; \quad (2.16)$$

where $T_{D6} = 2\pi g_s (2\pi)^7$ is the six-brane tension and h is the determinant of the metric on the round unit two-sphere. Recall that U is a function of ρ both explicitly and through its

dependence on $r(\)$. Hence the equation of motion for $r(\)$ is

$$\frac{d}{d} \left(1 + \frac{U_{KK}}{4^3} \right)^2 \frac{r}{1 + \underline{r}^2} = \frac{3}{2} \frac{U_{KK}}{5} \left(1 + \frac{U_{KK}}{4^3} \right)^2 r \frac{p}{1 + \underline{r}^2} : \quad (2.17)$$

Note that $r(\) = r_0$, where r_0 is a constant, is a solution in the supersymmetric limit ($U_{KK} = 0$), as in [6, 7]. This reflects the BPS nature of the system, which implies that there is no force on the D 6-brane regardless of its position in the 89-plane. In particular, then, the solution with $r_0 = 0$ preserves the $U(1)_A$ rotational symmetry in the 89-directions. If $U_{KK} \neq 0$ the force on the D 6-brane no longer vanishes and causes it to bend as dictated by the equation of motion above. We will see below that in this case there are no (physical) solutions that preserve the $U(1)_A$ symmetry.

If $U_{KK} \neq 0$, the analysis is facilitated by rescaling to dimensionless variables as follows:

$$! U_{KK} ; \quad r ! U_{KK} r ; \quad ! U_{KK} ; \quad (2.18)$$

in terms of which equation (2.17) becomes

$$\frac{d}{d} \left(1 + \frac{1}{4^3} \right)^2 \frac{r}{1 + \underline{r}^2} = \frac{3}{2} \frac{1}{5} \left(1 + \frac{1}{4^3} \right)^2 r \frac{p}{1 + \underline{r}^2} : \quad (2.19)$$

We seek solutions such that the asymptotic separation of the D 6-brane and the D 4-branes, L , is finite. That is, as $r \rightarrow 1$, $r(\) \rightarrow r_1$ with

$$r_1 = \frac{L}{U_{KK}} : \quad (2.20)$$

In the region $r \gg 1$ we have $\underline{r} \rightarrow 0$ and $r \rightarrow r_1$. Under these conditions we can linearize equation (2.19) with the result

$$\frac{d}{d} \underline{r} \sim \frac{3}{2} \frac{1}{3} r ; \quad (2.21)$$

the solution to which is

$$r(\) = A \frac{1}{p=J_{1=3}} \frac{2^{1=2} 3^{1=2}}{3=2} + B \frac{1}{p=J_{1=3}} \frac{2^{1=2} 3^{1=2}}{3=2} ; \quad (2.22)$$

where J are Bessel functions and A and B are arbitrary constants. For large r , the function multiplied by A tends to a constant, whereas that multiplied by B behaves as $1/r$. This means that for large r we have

$$r(\) \sim r_1 + \frac{C}{r} ; \quad (2.23)$$

where the constants r_1 and C are related to the quark mass and the chiral condensate, as we now show.

The bare quark mass is given by the string tension times the asymptotic distance between the D 4- and the D 6-brane.³ Taking (2.20) into account, we have

$$m_q = \frac{L}{2 \sqrt{s}} = \frac{U_{KK} r_1}{2 \sqrt{s}} : \quad (2.24)$$

The quark condensate can now be computed using a simple argument. The Hamiltonian density of the theory can be written as

$$Z \\ H = H_0 + m_q \int d^2 Q \bar{Q} ; \quad (2.25)$$

where H_0 is m_q -independent, and \bar{Q}, Q represent the hypermultiplet superfields in $N = 1$ notation. It follows that

$$\frac{E}{m_q} = h \int d^2 Q \bar{Q} i = h i ; \quad (2.26)$$

where $E = h i$ is the vacuum energy density. In the last equality, we have assumed that the vacuum expectation value of the fundamental scalars vanishes, since they are massive (even with $m_q = 0$ after supersymmetry breaking), that is, the energy density increases if they acquire a non-zero expectation value.

Since in the string description the quark mass is given by the asymptotic position of the D 6-brane, we need to evaluate the change in energy of the D 6-brane associated to a change of the boundary condition r_1 . In view of (2.16) this is given by

$$Z \\ E = \int d^2 x L = T_{D6} U_{KK}^3 \int d^2 x \frac{p}{h} \frac{1}{1 + \frac{1}{4^3}}^2 p \frac{1}{1 + \frac{r^2}{4^2}} ; \quad (2.27)$$

where L is the D 6-brane Lagrangian density rescaled in accordance with (2.18). Using the equations of motion this becomes

$$E = 4 \int d^2 x \frac{p}{h} \frac{1}{1 + \frac{1}{4^3}}^2 p \frac{r}{1 + \frac{r^2}{4^2}} = 4 T_{D6} U_{KK}^3 \int d^2 x \frac{r}{1 + \frac{r^2}{4^2}} = 4 T_{D6} U_{KK}^3 c ; \quad (2.28)$$

where we used (2.23) and the fact that $r|_{r=0} = 0$, by rotational symmetry in the 567-directions. In view of (2.24) we finally obtain

$$h i = \frac{E}{m_q} = 8 \frac{2 \sqrt{s} T_{D6} U_{KK}^2}{N_c} c : \quad (2.29)$$

As anticipated, the quark condensate is directly related to c ; we will see below that c is determined by r_1 . Note that, in terms of gauge theory quantities,

$$\frac{1}{N_c} h i' g_{YM}^2 N_c M_{KK}^3 c : \quad (2.30)$$

³This mass is trivially derived for the brane array (1.1) asymptotically at space. With supersymmetry ($U_{KK} = 0$), this bare mass persists in the decoupling limit and is then inherited by the compactified theory with supersymmetry-breaking boundary conditions, since setting $U_{KK} \neq 0$ does not alter the asymptotic properties of the model that, as usual in AdS/CFT-like dualities, determine the gauge theory parameters.

The normalization on the left-hand side is that expected in the 't Hooft limit.

We now return to the full equation of motion (2.19), which we will solve. In order to understand the nature of the solutions better, however, it is helpful to first consider the limit $r_1 \gg 1$, in which (approximate) analytical solutions can be found.

If $r_1 \gg 1$, the entire D 6-brane should lie far away from the 'bolt' at the center of the D 4-soliton, hence we expect the solution to be a small perturbation around the solution for $U_{KK} = 0$. In other words, we set $r(\zeta) = r_1 + r(\zeta)$ and assume that $r \gg 1$. Substituting this into (2.19) and expanding to linear order in r we find

$$\frac{d}{d\zeta} r^2 \approx \frac{3}{2} r^2 \frac{r_1}{r^2 + r_1^2} ; \quad (2.31)$$

which is easily integrated with the result

$$r \approx \frac{3r_1}{2} \int_0^{\zeta} \frac{dx}{(x^2 + r_1^2)^{5/2}} = \frac{1}{2r_1} \frac{1}{r^2 + r_1^2} ; \quad (2.32)$$

Here we have imposed the boundary condition $r = 0$ at $\zeta = 0$, as required by regularity of the solution at the origin of the 567-space. Integrating once more, with the boundary condition $r|_{\zeta=1} = 0$, we find

$$r(\zeta) \approx r_1 + \frac{1}{2r_1} \frac{1}{r^2 + r_1^2} ; \quad (2.33)$$

From this large r_1 solution, we see that the D 6-brane bends 'outwards', that is, it is 'repelled' by the D 4-branes. This repulsion persists for arbitrary values of r_1 , as is confirmed by numerical analysis. Eq. (2.19) can be integrated numerically for any value of r_1 , and we have plotted solutions for several values of r_1 in Figure 1.

Figure 2 displays the function $c(r_1)$ found by numerical integrations. As mentioned above, the value of r_1 together with the requirement of regularity at $\zeta = 0$ (i.e., $r|_{\zeta=0} = 0$) determines the solution completely. Hence choosing r_1 fixes $c = c(r_1)$. Recalling eqs. (2.24) and (2.29), which relate r_1 and c to the quark mass and condensate, respectively, we see that this corresponds precisely to what is expected on field-theoretic grounds: once the quark mass is specified, the infrared dynamics determines the chiral condensate. In the field theory we expect the $U(1)_A$ symmetry to be spontaneously broken by a non-zero condensate in the limit $m_q \rightarrow 0$. This is indeed confirmed by the numerical results for the D 6-brane embedding, since we see that, in Figure 2, $c(r_1)$ approaches a finite constant in the limit $r_1 \gg 1$. In this limit, the asymptotic boundary condition on the D 6-brane respects the rotational symmetry in the 89-plane, but it is energetically favourable for the D 6-brane to bend out in the 89-plane. Hence the embedding spontaneously breaks this rotational symmetry, which matches the $U(1)_A$ symmetry-breaking in the field theory.

We see from (2.33) that $c(r_1) \approx 1/(2r_1)$ for large r_1 , which is confirmed by the numerical results. This implies that the chiral condensate scales as $1/m_q$ for large m_q , as expected

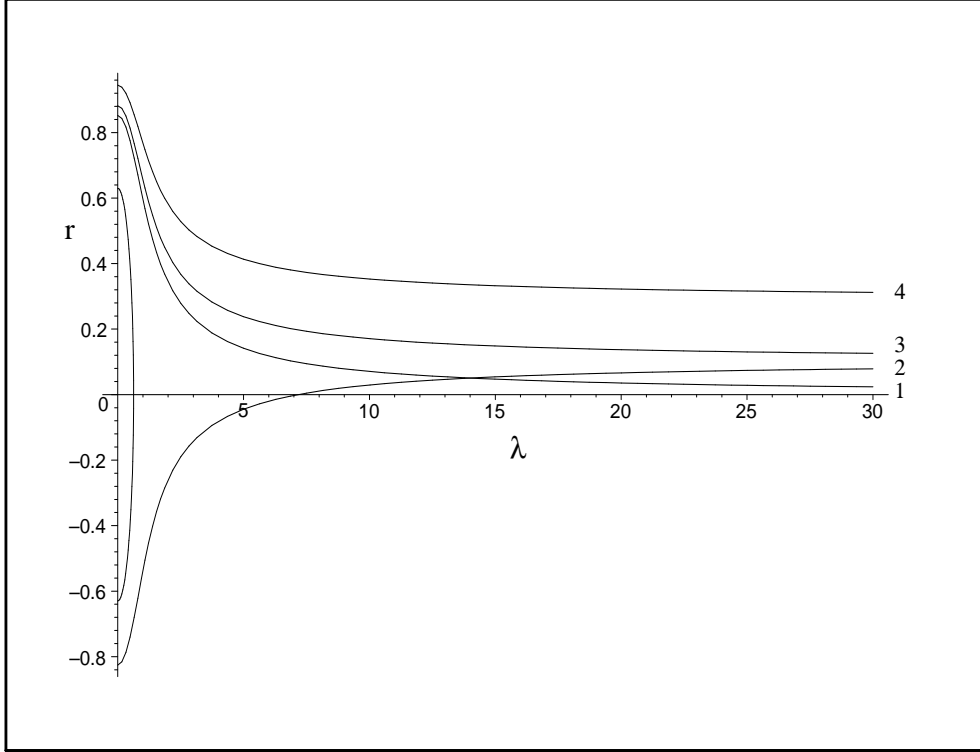


Figure 1: The D 6-brane embedding for several values of the quark mass m_q / r_1 . The interior of the 'circle' in the center is the region $U < U_{KK}$, which is actually not part of the space. The '2' and '3' embeddings correspond to the same value of r_1 but have opposite sign c 's; the '3' embedding has lower energy.

on field theory grounds [16]. A quick, somewhat heuristic argument for this in QCD is as follows.⁴ The trace of the energy-momentum tensor reads

$$T = m_q \frac{s(11N_c - 2N_f)}{24} TrF^2; \quad (2.34)$$

where we have explicitly written down the classical contribution, as well as the anomalous one coming from the one-loop beta-function. In the limit $m_q \rightarrow 1$ the theory resembles QCD with no quarks, for which

$$T = \frac{11N_c}{24} s TrF^2; \quad (2.35)$$

Taking vacuum expectation values and equating the two expressions we find

$$h \cdot i = \frac{sN_f}{12m_q} hTrF^2i; \quad (2.36)$$

Assuming that $hTrF^2i \neq 0$ we conclude that $h \cdot i / 1 = m_q$.

⁴We thank D.T.Son for explaining this point to us.

For each value of $r_1 > 0$, the numerical analysis actually finds two regular solutions, which have c 's of opposite sign. The curves labelled '2' and '3' in figure 1 are a representative example of such a pair of solutions.⁵ We have confirmed that the solutions with positive c , for which $r(\phi) > 0$ for all ϕ (e.g., curve 3), have the lower energy density. The negative- c solutions bend around the opposite side of the bolt at the center of the D 4-soliton geometry. Naively, these solutions should be unstable, since the D 6-brane is free to 'slide off the bolt' by moving out of the $\phi = 0$ plane, and relax to the lower-energy, positive- c solution. We will return to this issue in the next section, where we study fluctuations of the D 6-brane worldvolume fields around embedding solutions of each type | in fact, we will find tachyonic fluctuations for the negative- c solutions, confirming the intuition given above.

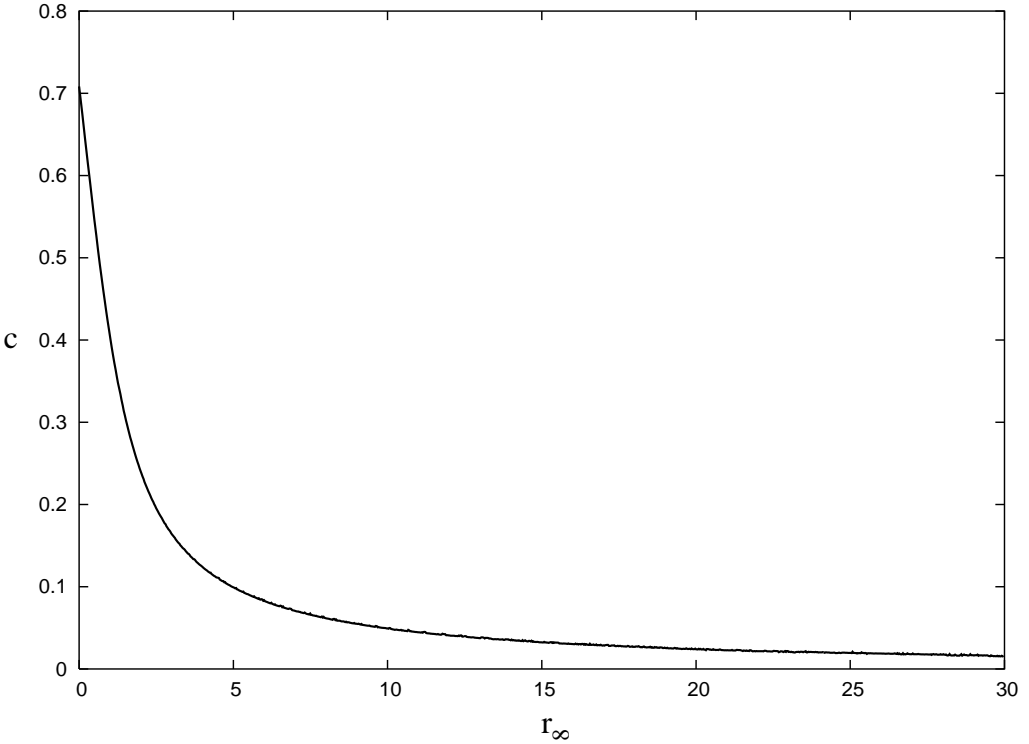


Figure 2: The quark condensate h_i/c as a function of the quark mass m_q/r_1 .

Note that $r(\phi) = 0$ is an exact mathematical solution of eq. (2.17) even if $U_{KK} \neq 0$. Therefore one might be tempted to conclude that it provides an alternative, $U(1)_A$ -preserving solution whose energy should be shown to be higher than that of the $U(1)_A$ -breaking solution above in order to establish spontaneous chiral symmetry breaking. However, the solution $r(\phi) = 0$ is not physically acceptable if $U_{KK} \neq 0$ because it corresponds to an open D 6-brane. That is, this solution yields a D 6-brane with a boundary, which is forbidden by charge conservation. The boundary is easily seen as follows. With $r(\phi) = 0$ we have $\phi = \pi$, so

⁵To describe the second solution (curve 2), we allow $r(\phi) < 0$ and restrict ϕ to the range $[0; \pi]$.

this solution term inates at the origin of the U -plane, that is, at $U = U_{KK}$. Since, at this point, the S^2 in the metric (2.15) still has a nite radius, $R^{3=4}U_{KK}^{1=4}$, the D 6-brane would have an $R^{1=3}S^2$ -boundary if it inated at $U = U_{KK}$. Note that if $U_{KK} = 0$ then the two-sphere radius shrinks to zero-size and the six-brane closes o at $U = 0$. Hence the $U(1)_A$ -preserving solution $r(\) = 0$ is physically sensible in the supersymmetric case. This result is in agreement with the fact that unbroken supersymmetry forbids a non-zero chiral condensate. Note, however, that this is only a formal argument, since in the limit $U_{KK} \rightarrow 0$ the curvature at $U = U_{KK}$ diverges, meaning that the supergravity description cannot be trusted in this region [11].

In section 7, we will see that the solution $r(\) = 0$ can play a role in the case $U_{KK} \neq 0$ if it is simply extended past the origin of the U -plane. The physical interpretation of such a solution is not that of a D 4/D 6 intersection, but rather that of a D 4/D 6/ $\overline{D}6$ intersection.

3. Meson spectroscopy from D 6-brane fluctuations ($N_f = 1$)

Here, we consider a certain class of fluctuations of the D 6-brane around the embeddings described in the previous section. We consider rst the positive-c (negative-condensate) embeddings, which were argued to be stable and so should correspond to the true 'vacuum state' for a given quark mass. For simplicity we restrict ourselves to fluctuations of the scalar elds r and ϕ , as these are su cient to illustrate the physics we wish to exhibit. In the dual gauge theory, these fluctuations correspond to a class of scalar mesons. Therefore we are considering embeddings of the D 6-brane of the form

$$= 0 + \dots ; \quad r = r_{vac}(\) + \delta r ; \quad \phi = \text{constant} ; \quad (3.1)$$

where the fluctuations δr and ϕ are functions of all of the worldvolume coordinates and $r_{vac}(\)$ is the numerically-determined vacuum embedding of the previous section.

In corroboration of our previous argument for the stability of these embeddings, we nd, in particular, that the spectra of these fluctuations are non-tachyonic. We also brie y consider fluctuations around the negative-c (positive-condensate) embeddings and show their spectra do contain tachyonic modes, making manifest the instability of these con gurations.

3.1 Analysis of the spectrum

Using the background metric (2.14) with the rescalings (2.18), the pullback of (2.14) to the embedding given in (3.1) is

$$\begin{aligned} ds^2 = & \frac{U}{R}^{3=2} dx^a dx^b + K [(1 + \frac{r^2}{r_{vac}^2}) d^2 + \frac{1}{2} d^2 + 2r_{vac} \partial_a(r) d dx^a] \\ & + K \partial_a(r) \partial_b(r) dx^a dx^b + (r_{vac} + r)^2 \partial_a(\phi) \partial_b(\phi) dx^a dx^b ; \end{aligned} \quad (3.2)$$

where a and b run over all of the worldvolume directions. To quadratic order in fluctuations, the D 6-brane Lagrangian density is then

$$L = L_0 + T_6 U_{KK}^3 \frac{2P}{h} \frac{P}{1 + \frac{r_{vac}^2}{r^2}} \left(\frac{3(7 \frac{r_{vac}^2}{r^2})^2}{16 \frac{10}{r_{vac}}} + \frac{3(4r_{vac}^2)^2}{4 \frac{7}{r_{vac}}} (r)^2 \right. \\ \left. + \frac{3r_{vac}}{4 \frac{5}{r_{vac}}} \frac{1}{1 + \frac{1}{4 \frac{3}{r_{vac}}}} \frac{r_{vac} @ (r^2)}{1 + \frac{r_{vac}^2}{r^2}} \right) \\ + \frac{1}{1 + \frac{1}{4 \frac{3}{r_{vac}}}} \frac{2}{a} \frac{X}{2g_{aa}} \frac{[\partial_a(r)]^2}{1 + \frac{r^2}{r_{vac}}} + r_{vac}^2 [\partial_a(r)]^2 ; \quad (3.3)$$

where L_0 is the Lagrangian density evaluated for the vacuum embedding, as in eq. (2.16). Here, $\frac{r^2}{r_{vac}} = \frac{r^2}{r_{vac}^2} + r_{vac}^2$ and the g_{aa} in the last line correspond to the metric coefficients from eq. (2.15). In particular then, they contain no dependence on the fluctuations. Of course, integration by parts and the equation of motion (2.17) for r_{vac} allowed the terms linear in r to be eliminated.

The linearised equations of motion that follow are, for r :

$$\frac{9}{4M_{KK}^2} \frac{r_{vac}^2}{\frac{3}{r_{vac}}} \frac{1}{1 + \frac{1}{4 \frac{3}{r_{vac}}}} \stackrel{4=3}{=} @ @ (r) + \frac{r_{vac}^2}{2} \frac{1}{1 + \frac{1}{4 \frac{3}{r_{vac}}}} \stackrel{2}{r^2} (r) \\ + \frac{1}{2P} \frac{d}{1 + \frac{r_{vac}^2}{r^2}} \frac{d}{P} \frac{r_{vac}^2}{1 + \frac{r_{vac}^2}{r^2}} \frac{1}{1 + \frac{1}{4 \frac{3}{r_{vac}}}} \stackrel{2}{r^2} (r) = 0 ; \quad (3.4)$$

and, for r :

$$\frac{2}{P} \frac{d}{1 + \frac{r_{vac}^2}{r^2}} \frac{9}{4M_{KK}^2} \frac{1}{\frac{3}{r_{vac}}} \frac{1}{1 + \frac{1}{4 \frac{3}{r_{vac}}}} \stackrel{4=3}{=} @ @ (r) + \frac{1}{2} \frac{1}{1 + \frac{1}{4 \frac{3}{r_{vac}}}} \stackrel{2}{r^2} (r) \\ + \frac{d}{d} \frac{2}{(1 + \frac{r_{vac}^2}{r^2})^{3=2}} \frac{1}{1 + \frac{1}{4 \frac{3}{r_{vac}}}} \stackrel{2}{r^2} (r) \frac{d}{d} \frac{3}{2} \frac{r_{vac}^2}{M_{KK}^2} \frac{r_{vac}}{1 + \frac{r_{vac}^2}{r^2}} \frac{1}{1 + \frac{1}{4 \frac{3}{r_{vac}}}} \stackrel{2}{r^2} (r) \\ 2P \frac{r_{vac}^2}{1 + \frac{r_{vac}^2}{r^2}} \frac{3(7r_{vac}^2)^2}{8 \frac{10}{r_{vac}}} + \frac{3(4r_{vac}^2)^2}{2 \frac{7}{r_{vac}}} \quad r = 0 : \quad (3.5)$$

In these expressions, r^2 is the Laplacian on the two-sphere.

From the form of the equations of motion, it is clear that we may separate variables to write

$$= P(r) e^{ik_r} \times Y_m(S^2) ; \quad r = R(r) e^{ik_r} \times Y_{m_r}(S^2) ; \quad (3.6)$$

where Y_m are the conventional spherical harmonics. We then look for normalizable solutions with definite S^2 -angular momentum λ_r and four-dimensional mass $M_{,r}^2 = k_{,r}^2$. For the sake of simplicity in the following, we only focus on the case $\lambda_r = 0$ and find the lowest-mass modes for each fluctuation.

We employ the shooting method to solve the linearized equations of motion. First we use the asymptotic form of the equations for $r \gg 1$ and the requirement of normalizability

to determine the asymptotic boundary conditions for the fluctuations. Then we vary the four-dimensional mass parameters until, by numerically integrating the equation of motion, we find solutions that are also regular at the origin. Recall⁶ that the asymptotic behaviour of the vacuum profile is $r_{\text{vac}}' \Big|_{r=0} = 0$, where r_1 is related to the quark mass by equation (2.24). In this asymptotic region we have that $r_{\text{vac}}(0) \neq 0$, so the equation of motion for becomes, approximately,

$$\frac{9M^2}{4M_{\text{KK}}^2} \frac{r_{\text{vac}}^2}{r} (r) + \frac{d}{d} r_{\text{vac}}^2 \theta(r) = 0; \quad (3.7)$$

and similarly that for r becomes

$$\frac{9M^2}{4M_{\text{KK}}^2} \frac{1}{r} (r) + \frac{d}{d} r^2 \theta(r) = 0; \quad (3.8)$$

It follows that the asymptotic behaviour of $r(r)$ does not depend on that of $r_{\text{vac}}(r)$, whereas that of $\theta(r)$ depends crucially on whether or not $r_1 = 0$, that is, whether or not the quarks are massless. We will now show that if $r_1 = 0$ then there exists a normalizable mode with $M = 0$, whereas if $r_1 \neq 0$ there is a mass gap in the spectrum.

If we set $r_1 = 0$, we find that the asymptotic equation for becomes

$$\frac{9M^2}{4M_{\text{KK}}^2} \frac{1}{r^3} (r) + \theta^2(r) = 0; \quad (3.9)$$

The first term is sub-leading for large r , so we may drop it to find that the asymptotic form of $\theta(r)$, regardless of the value of M , is

$$\theta(r) \sim b + a/r; \quad (3.10)$$

where a and b are arbitrary constants. For $r_1 \neq 0$, however, we find that

$$\frac{9M^2}{4M_{\text{KK}}^2} \frac{1}{r^3} (r) + \frac{2}{r} \theta(r) + \theta^2(r) = 0; \quad (3.11)$$

Again the first term is sub-leading for large r , so the solution is

$$\theta(r) \sim a + b/r; \quad (3.12)$$

Normalizable solutions correspond to the boundary conditions $a = 0$ and $b = 0$ in the cases $r_1 = 0$ and $r_1 \neq 0$, respectively, since the terms with coefficients b and b are the ones that fall off more rapidly at infinity. Since the differential equations we are solving are linear, we may choose $b = 0$ without loss of generality, so we are left with the boundary conditions $f = 1$; $\theta = 0$ if $r_1 = 0$, and $f = 1$; $\theta = 1 = 1/r^2$ if $r_1 \neq 0$. A similar analysis for the fluctuations shows that they obey the same asymptotic equation of motion as the fluctuations in the $r_1 \neq 0$ case, so the appropriate boundary conditions are $f(r=1) = 1$; $\theta(r=1) = 1/r^2$.

⁶Also recall that we are working with dimensionless variables r and θ , rescaled as in eq. (2.18).

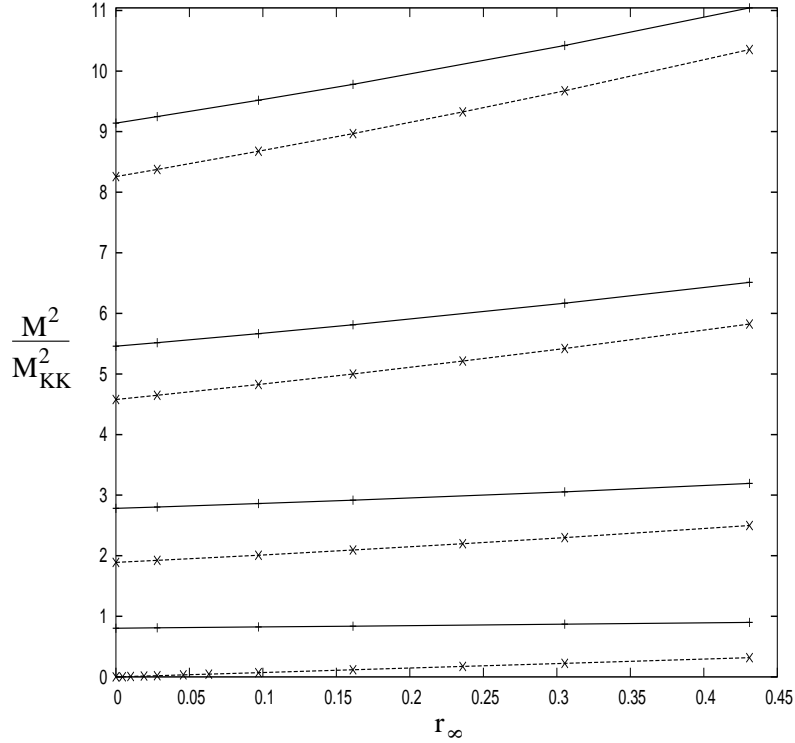


Figure 3: Squared masses for the four lowest-lying r -modes (dashed lines), and the four lowest-lying r -modes (solid lines), as functions of the quark mass m_q / r_1 .

Now note that $\psi = e^{ik\cdot x}$, with $k^2 = 0$, is an exact, regular solution of (3.4) with zero four-dimensional mass (and $r^2(\psi) = 0$), which is normalizable only if $r_1 = 0$. This means that with massless quarks there is a massless meson in the spectrum of the gauge theory, the dual of which is the zero-m mode fluctuation of the D6-brane field. That is, the mathematical form of these fluctuations shows that they correspond to rotations of the vacuum embedding in the 89-plane. Of course, this form is precisely as expected for the Goldstone mode associated with the spontaneous breaking of this rotational symmetry.

The shooting technique allows us to verify this numerically, and to find the values of $M_{r,x}$ for which other normalizable, regular solutions exist. The results are the low-lying scalar meson spectra, which are displayed in Figure 3 for different values of the quark mass. As anticipated, there is no mass gap in the r -meson spectrum when the quark is massless. There is a smooth transition to a theory with a mass gap as the quark mass is increased and, in fact, a best-fit (shown in Figure 4a) yields a linear relationship,⁷ $M^2 \approx 0.73 M_K^2 r_1$, for small r_1 / m_q , as expected from the GOMR relationship (1.2), which we will reproduce analytically in the next section.

As shown in Figure 3, there are no normalizable, regular solutions of equation (3.5) with $M_r = 0$, so there is a mass gap in the r -meson spectrum regardless of the value of the quark

⁷A n analogous relationship was observed in [9].

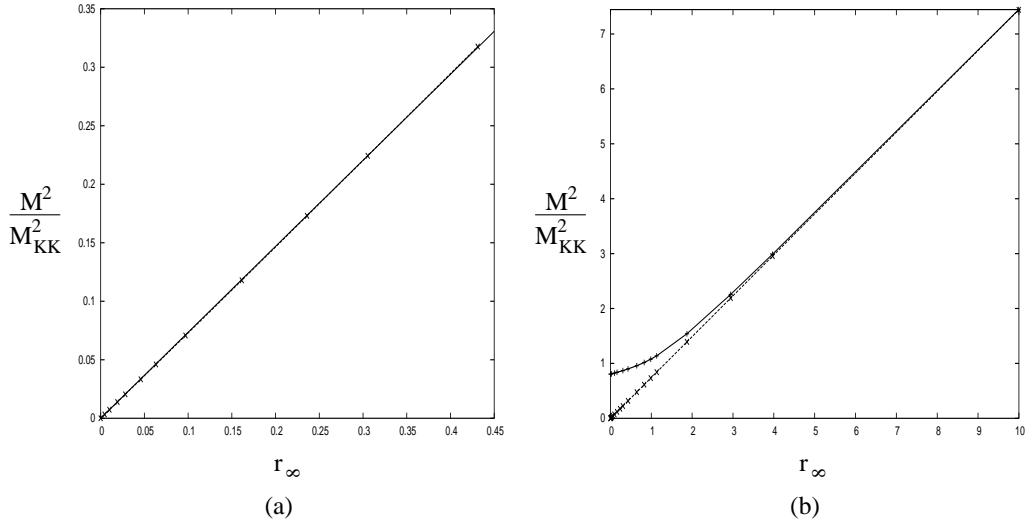


Figure 4: (a) Linear fit of the lowest-lying mode for different values of m_q . (b) Degeneracy of the lowest-lying (dashed) and r (solid) modes in the supersymmetric limit $m_q = 1$.

mass. For small quark mass the mass scale of all of the mesons, except the lowest-lying mode, is⁸

$$M^2 - M_{KK}^2 - \frac{U_{KK}}{R^3} : \quad (3.13)$$

This is another reflection of the lack of decoupling between the QCD scale and the compactification scale.

As suggested by Figure 3, the r -and r -mesons occur in pairs that become degenerate for large enough a quark mass. The reason is that, in the supersymmetric case ($U_{KK} = 0$), these mesons belong to the same supermultiplet and hence have equal masses, as in [7]. If $U_{KK} \neq 0$ this degeneracy is only approximate for quark masses much larger than the supersymmetry-breaking scale, M_{susy} , becoming exact in the limit $m_q \gg 1$. Geometrically, this corresponds to the fact that the distortion of the D6-brane away from the flat, supersymmetric profile decreases the farther away from the D4-branes we embed it. Since this distance scale is measured by L / m_q , and U_{KK} characterises the supersymmetry breaking, we expect that, for $L \gg U_{KK}$, the characteristic mass scale of the mesons should become independent of U_{KK} and depend, instead, on some ratio of L and R . To see that this is indeed the case, we approximate the vacuum profile by the flat solution in equations (3.4) and (3.5), that is, we set $r_{vac}(r) = r_1$, and we expand these equations assuming that $r_1 \gg 1$. In terms of a new variable $y = r/L$ we obtain (for zero S^2 -angular momentum)

$$\frac{R^3 M^2}{L (y^2 + 1)^{3/2}} + \frac{1}{y^2} \frac{d}{dy} [y^2 \partial_y] = 0 ; \quad (3.14)$$

⁸This also sets the scale of the glueball mass spectrum [3].

and

$$\frac{R^3 M_r^2}{L(y^2 + 1)^{3/2}} r + \frac{1}{y^2} \frac{d}{dy} [y^2 \partial_y r] = 0 : \quad (3.15)$$

The fact that the two types of fluctuations satisfy the same equation means that the spectrum becomes degenerate in this limit. It is also clear that the mass scale for the mesons in this limit is now

$$M^2 = \frac{L}{R^3} = \frac{m_q M_{KK}}{g_{YM}^2 N_c} ; \quad (3.16)$$

since this is the only scale that appears in eq. (3.14), (3.15).

The transition between the regimes (3.13) and (3.16) occurs at $L = U_{KK}$, and is illustrated for the lightest r - and m mesons in figure 4b, which was generated by solving equations (3.5) and (3.4) numerically. The figure clearly illustrates the degeneracy of the modes in the expected regime. The condition $L = U_{KK}$ translates into $m_q = M_{susy}$, with M_{susy} as defined in (1.4), so M_{susy} is indeed the scale at which supersymmetry is restored, as suggested by our choice of notation. Note that at the transition point, at which of course eqs. (3.13) and (3.16) coincide, we have $M = m_q = (g_{YM}^2 N_c)^{1/2}$. As we are working in the 't Hooft limit of the gauge theory, these mesons are very deeply bound, i.e., $M \ll 2m_q$. The suppression of these meson masses by the 't Hooft coupling is even stronger than that found in a similar context in [7], where $M = m_q = \frac{p}{g_{YM}^2 N_c}$. For large quark mass there is an extra suppression implicit in eq. (3.16) due to the fact that M^2 scales linearly in m_q , as opposed to quadratically.

As we are working in a range where we expect the gauge theory is $ve\text{-dim}\text{ensional}$, it is perhaps more appropriate to re-express the transition scale in terms of the $ve\text{-dim}\text{ensional}$ gauge coupling; it then reads $m_q = \frac{g^2 N_c M_{KK}^2}{M_{susy}^2}$. Similarly, the mass scale typical of the mesons becomes $M^2 = m_q = (g_5^2 N_c)^{1/2}$. In any event, the transition scale suggests that the effective mass squared of some of the microscopic degrees of freedom must be at least of the order M_{susy}^2/M_{KK}^2 , rather than just M_{KK}^2 . Note that this mass scale is a factor of $\frac{p}{g_{YM}^2 N_c}$ larger than that coming from a simple one-loop calculation for the scalar masses, which yields $\frac{g_{YM}^2 N_c M_{KK}^2}{M_{susy}^2}$. This factor seems to be ubiquitous in extrapolations from weak to strong 't Hooft coupling in the context of AdS/CFT.

As we saw above, the squared masses of all mesons scale linearly in the quark mass as $m_q \ll 1$. For the lightest meson, the results displayed in figure 4b seem to indicate that, in fact, this linear relationship is valid not only in the limits of small and large m_q , but for all quark masses. This result has been confirmed to within the best accuracy of our numerical analysis. Unfortunately, eq. (3.14) has four regular singular points and so no closed-form analytic solution is available, but its numerical solution gives, for the lowest-mass modes,

$$M^2 = 1.66 \frac{L}{R^3} = 20.91 \frac{M_{KK}}{g_{YM}^2 N_c} m_q = 0.74 M_{KK}^2 r_1 : \quad (3.17)$$

The final form of this expression agrees with a best-fit of the data plotted in the region of figure 4b with $r_1 \ll 1$ and, in principle, describes the extension of this figure to arbitrarily high values of r_1 . We therefore conclude that, in our model, the GMR linear relation between M^2 and m_q extrapolates to all quark masses.

3.2 Stability Issues

Recall that, at the end of section 2, we remarked that our numerical integrations had revealed two classes of six-brane embeddings, those with positive c and those with negative c . From the numerical analysis, we could show that, for a given r_1 , the positive- c or negative-condensate solutions had the lower energy density. Furthermore we argued that the negative- c solutions should be unstable.

The stability of the negative-condensate (positive- c) vacuum embedding is reflected in the fact that the spectrum of fluctuations does not contain tachyonic modes. While numerical searches did not reveal any tachyonic fluctuations, one can formulate a general argument that no such modes can exist in the spectrum of ⁹. Consider the equation of motion (3.4) (with zero angular momentum on the two-sphere, for simplicity). Multiplying by ∂_r , integrating over r and integrating by parts, yields

$$\begin{aligned} \int_0^1 d\tau \left(\frac{9M^2}{4M_{KK}^2} \frac{r_{vac}^2}{3} \frac{1}{1 + \frac{1}{4} \frac{r_{vac}^3}{3}} \frac{d}{d\tau} \frac{1 + \frac{1}{4} \frac{r_{vac}^3}{3}}{1 + \frac{r_{vac}^2}{1 + \frac{1}{4} \frac{r_{vac}^3}{3}}} \frac{d}{d\tau} \frac{1 + \frac{1}{4} \frac{r_{vac}^3}{3}}{1 + \frac{r_{vac}^2}{1 + \frac{1}{4} \frac{r_{vac}^3}{3}}} \right) \\ = \frac{p}{1 + \frac{r_{vac}^2}{1 + \frac{1}{4} \frac{r_{vac}^3}{3}}} \Big|_0^1 = 0 : \end{aligned} \quad (3.18)$$

Note that we were able to set the term on the right-hand side to zero using the behaviour of the normalizable modes at $\tau = 0$ and $\tau = 1$. On the left-hand side, the second term in the integrand is manifestly negative or zero, while the sign of the first term depends on that of M^2 . Therefore, for tachyonic modes it is clear that the integral will be negative definite, which is inconsistent with the vanishing of the right-hand side. The argument extends to include nonvanishing ∂_r , which simply introduces an additional negative-definite term under the integral. Hence we conclude that the negative-condensate embeddings are free from tachyonic instabilities in this sector. As this was the sector with the lowest lying mode, we might have expected it to be the most potentially problematic with regards to stability. Hence we are confident that these positive- c solutions are stable.

Now we turn our attention to the negative- c or positive-condensate embeddings. Recall that our intuition was that these solutions should be unstable to 'sliding off the bolt'. Since the embedding coordinate (r , here) always vanishes at some value of τ for this case, we cannot address the issue of such an instability using the equation of motion, since r is not everywhere well-defined. Hence, we change to Cartesian coordinates X and Y in the r -plane. With the choice that the D6-brane lies at $r_{vac}(\tau) = r_0 = 0$ (i.e., $Y_{vac}(\tau) = 0$), it follows that the embedding profile in X satisfies the equation of motion (2.19) and we may set $X_{vac}(\tau) = r_{vac}(\tau)$. Fluctuations in $Y(\tau)$ are now the modes relevant for stability and have the benefit of being well-defined for all τ . One finds the following equation of motion for

⁹We expect that these arguments extend to r fluctuations but we did not explicitly consider these modes a possible decay channel between the two D6-brane embeddings, due to the geometric obstruction provided by the 'bolt' at the centre of the D4-soliton.

these fluctuations:

$$\frac{9}{4M_{KK}^2} \frac{1}{3_{vac}} \left(1 + \frac{1}{4} \frac{3_{vac}}{2_{vac}} \right)^{4=3} \Theta(0) (Y) + \frac{1}{2} \left(1 + \frac{1}{4} \frac{3_{vac}}{2_{vac}} \right)^2 r^2 (Y) \\ + \frac{1}{2} \frac{1}{1 + X_{vac}^2} \frac{d}{d} \left(4 \frac{2}{1 + X_{vac}^2} \right) \left(1 + \frac{1}{4} \frac{3_{vac}}{2_{vac}} \right)^2 \Theta(Y)^5 + \frac{3(1 + 4 \frac{3_{vac}}{2_{vac}})}{8} Y = 0; \quad (3.19)$$

where, now, $\frac{2_{vac}}{3_{vac}} = \frac{2}{2} + X_{vac}^2$. Making a stability argument along the lines of that given above for α is no longer possible, due to the presence of the final term in (3.19). This term introduces into the integrand analogous to that in eq. (3.18) a contribution that is manifestly positive. Hence this approach does not yield a definite conclusion in this case.

However, it is still possible to look directly for tachyonic modes in the spectrum of fluctuations around the negative-condensate embeddings using our numerical techniques. From eq. (3.19) one can deduce the asymptotic behaviour of the Y modes to be

$$Y \propto \alpha + \beta r; \quad (3.20)$$

independent of the vacuum embedding. Using the shooting method as before, the spectrum of each positive-condensate embedding considered numerically is found to contain a tachyonic mode and, furthermore, these modes become more tachyonic as the quark mass increases | see figure 5. As is suggested in the figure, the squared mass of the lowest-lying Y mode has a linear dependence on the quark mass. In fact, a best-fit of the data gives $M_Y^2 \approx 0.72 M_{KK}^2 r_1$.

An examination of the next-to-lowest-lying Y mode (not shown in the figure) indicates that the mass of this mode, which is real and positive for $m_q = 0$, also decreases as a function of r_1 . So for sufficiently large quark mass the spectrum may contain more than one tachyon. However, we could not confirm this directly because for large r_1 the negative-condensate embeddings approach extremely close to the bolt, and our computer code behaved erratically in this situation.

4. The pseudo-Goldstone boson

As discussed in the previous section, if $m_q = 0$ the spectrum contains a massless mode that can be understood as the Goldstone boson of the spontaneously broken $U(1)_A$ symmetry.

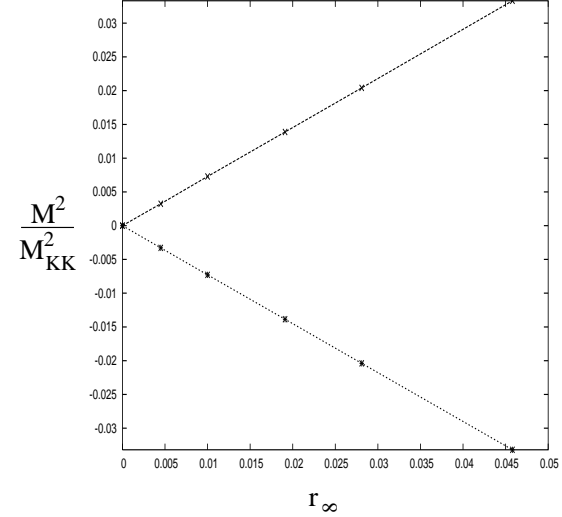


Figure 5: The lowest-lying mode for some negative-condensate embeddings (upper line), and the lowest-lying Y mode for the corresponding positive-condensate embeddings (lower line) | the Y modes are tachyonic.

This is akin to the 0 meson in QCD, which is massless in the large- N_c limit. In an abuse of language, however, we will refer to this Goldstone boson as a 'pion'. For non-zero quark mass, the $U(1)_A$ symmetry is explicitly broken and the pion becomes a pseudo-Goldstone boson with a mass M that, according to our numerical analysis, grows as $M^2 \sim m_q$. This means that at low energies, $E \ll M$, the dynamics is dominated by this particle. In this section we will provide an analytic proof, using the string description, that the pion's mass actually obeys the well-known Goldstone-Banerjee relation (1.2).

Recall that the gauge theory pion is dual to a fluctuation of the D6-brane of the form $\phi = e^{ik \cdot x} (\theta)$ that solves equation (3.4) with $r^2(\theta) = 0$, that is,

$$\frac{d}{d\theta} [\phi(\theta)'] = M^2 (\theta)'; \quad (4.1)$$

where $M^2 = k^2$ is the four-dimensional mass,

$$\phi(\theta) = r_{vac}^2 \frac{1}{1 + \frac{1}{4} \frac{r_{vac}^2}{\theta^3}} \frac{p}{1 + \frac{r_{vac}^2}{\theta^2}}; \quad (4.2)$$

$$(\theta) = \frac{9}{4M^2} \frac{r_{vac}^2}{\theta^3} \frac{1}{1 + \frac{1}{4} \frac{r_{vac}^2}{\theta^3}} \frac{4p}{1 + \frac{r_{vac}^2}{\theta^2}}; \quad (4.3)$$

and $\frac{2}{r_{vac}} = \theta^2 + r_{vac}^2$. The allowed solutions are those that both satisfy $\int j_0 = 0$ and are normalizable with respect to the scalar product

$$h' \int_0^{\theta_1} d\theta (\theta)'_1 (\theta)'_2 (\theta); \quad (4.4)$$

This defines an eigenvalue problem whose solution is a complete set of orthogonal eigenfunctions ψ_n with eigenvalues M_n^2 . Notice that if $\psi(\theta) = \text{constant}$ then the eigenvalue equation is satisfied with $M^2 = 0$, but the mode is normalizable only if $r_{vac}(\theta) \neq 0$ as $\theta \rightarrow 1$. If $\psi(\theta)$ is not constant, multiplying eq.(4.1) by ψ' , integrating both sides with respect to θ and performing an integral by parts in the left-hand side, we arrive at

$$M^2 = \frac{\int_0^{\theta_1} d\theta \psi(\theta)'^2}{\int_0^{\theta_1} d\theta (\psi')^2} > 0; \quad (4.5)$$

Since from (4.2) and (4.3), we have $\psi(\theta) > 0$ and $(\psi')^2 > 0$ it follows that M^2 is positive as indicated.¹⁰

Having said that, we now want to compute the mode with lowest eigenvalue $M^2 > 0$ when m_q is non-vanishing but small. That is, let us suppose that $r_{vac} \neq r_1$ as $\theta \rightarrow 1$, with r_1 small but non-zero. In this case we expect that the normalizable eigenmode can be obtained from the massless-quark zero-mode, namely $\psi(\theta) = \text{constant}$, by using perturbation theory. To this end, it is convenient to define

$$(\theta) = \frac{p}{\psi(\theta)'} \psi(\theta); \quad (4.6)$$

¹⁰This is not valid when r_{vac} vanishes at some point (which is not the case studied here) | see the more detailed discussion after equation (3.18).

which satisfies the new eigenvalue equation

$$- = M^2 ; \quad (4.7)$$

where $\bar{p} = \bar{p}$, and \bar{p} is the new integration measure. If $r_1 = 0$ then $\psi(r) = \psi(r)$ is a normalizable solution of (4.7) with zero eigenvalue. Making a small change in the boundary condition, $r_1 \neq 0$, induces a small change in the vacuum profile $r_{vac}(r)$, which in turn induces a small change in the functions $\psi(r)$ and $\psi(r)$ appearing in equation (4.7). Standard quantum mechanics perturbation theory can then be applied to obtain the new lowest eigenvalue.

Let us denote with a bar the quantities corresponding to $r_1 = 0$, so that for $r_1 \neq 0$ we have

$$\bar{\psi} = \psi + \delta\psi ; \quad (4.8)$$

$$\bar{p} = p + \delta p ; \quad (4.9)$$

where $\delta\psi$ and δp are the differences induced by the change in $r_{vac}(r)$. The new lowest eigenvalue and its associated wavefunction, $M^2 \neq 0$ and $\bar{\psi} = \psi + \delta\psi$, obey, to leading order,

$$- = M^2 ; \quad (4.10)$$

Decomposing ψ as a linear combination of massless-quark eigenfunctions, $\psi = \sum_{n=0}^{\infty} c_n \psi_n$, we obtain

$$\sum_{n=1}^{\infty} n M_n^2 \psi_n + - = M^2 ; \quad (4.11)$$

where we have dropped the first term in the series, using $M_0 = 0$. Multiplying by ψ_n , integrating over R^3 and using the orthogonality condition $\int_0^1 d\psi_n \psi_m = 0$ for $n > 0$ (since ψ_0 is the zero-mode eigenfunction and is real) we deduce that

$$M^2 \int_0^1 d\psi_1^2 = \int_0^1 d\psi_1^2 = \int_0^1 d\psi_1 (h - \sum_{i=1}^{\infty} \int_0^1 d\psi_i) = h - \sum_{i=1}^{\infty} \int_0^1 d\psi_i = 0 ; \quad (4.12)$$

Recalling that

$$h = r_{vac} \left(1 + \frac{1}{4} \int_{vac}^3 (1 + r_{vac}^2)^{-1/4} \right) ; \quad (4.13)$$

which implies

$$\begin{aligned} h &= r_{vac} \left(1 + \frac{1}{4} \int_{vac}^3 (1 + r_{vac}^2)^{-1/4} \right) = \frac{3}{4} \int_{vac}^5 (1 + r_{vac}^2)^{-1/4} r_{vac} \\ &= r_{vac} \left(1 + \frac{1}{4} \int_{vac}^3 \frac{1}{2} (1 + r_{vac}^2)^{-5/4} r_{vac}^2 \right) ; \end{aligned} \quad (4.14)$$

we see that the only contribution to the last term in equation (4.12) comes from $\epsilon = 1$. This is easily evaluated, since for large ϵ we have

$$r_{\text{vac}}' \underset{\epsilon \rightarrow \infty}{\sim} 0 - \frac{1}{2} ; \quad r_{\text{vac}}' \underset{\epsilon \rightarrow \infty}{\sim} 0 - \frac{1}{2} ; \quad (4.15)$$

It follows that the new eigenvalue is given by

$$M^2 = \frac{R_1^2 \frac{c}{d} \frac{n}{2}}{0} = \frac{R_1^2 \frac{c}{d} \frac{n}{2}}{0} ; \quad (4.16)$$

To show that this formula is precisely the G M O R relation (1.2), we need to identify the pion decay constant in the string description. In this description, a shift of the chiral angle that parametrizes the space of vacua related to each other by the $U(1)_A$ symmetry corresponds to a rigid rotation of the D 6-brane field (both take values between 0 and 2π). Similarly, the pion field is identified with the normalizable, massless mode ϵ , described in section 3.1. The pion decay constant can be read off from the normalization of the kinetic term in the four-dimensional low-energy effective Lagrangian for this mode. That is, we integrate the ϵ -term in eq. (3.3) over ϵ and the coordinates on S^2 and as a result find a four-dimensional action of the form

$$S = \frac{f^2}{2} \int d^4x \epsilon \partial_\mu \epsilon \partial_\nu \epsilon ; \quad (4.17)$$

where f is the pion decay constant. From eq. (3.3), then we have

$$\begin{aligned} f^2 &= T_{D6} U_{KK}^3 \int_0^{Z_1} d\epsilon \int_0^{Z_1} d\epsilon \int_0^{Z_1} d\epsilon \frac{9}{4M_{KK}^2} \frac{r_{\text{vac}}^2}{\epsilon^3} \frac{1}{1 + \frac{1}{4} \frac{r_{\text{vac}}^2}{\epsilon^3}} \frac{4=3 Q}{1 + r_{\text{vac}}^2} \\ &= 4 T_{D6} U_{KK}^3 \int_0^{Z_1} d\epsilon \epsilon \epsilon ; \end{aligned} \quad (4.18)$$

Combining this result with eqs. (2.24) and (2.29), we see that eq. (4.16) is precisely the G M O R relation (1.2), as anticipated.

We close this section by verifying the agreement between the analytical expression (4.16) above and the results obtained purely by numerical methods and displayed in figure 4a. The integral in equation (4.16) can be evaluated numerically with the result

$$\int_0^{Z_1} d\epsilon \epsilon = \frac{9}{4M_{KK}^2} \int_0^{Z_1} d\epsilon \epsilon \frac{2r_{\text{vac}}^2}{\epsilon^3} \frac{1}{1 + \frac{1}{4} \frac{r_{\text{vac}}^2}{\epsilon^3}} \frac{4=3 Q}{1 + r_{\text{vac}}^2} \frac{0.97}{M_{KK}^2} ; \quad (4.19)$$

Similarly, the numerical result for the constant c for zero quark mass (see Figure 2) is $c' = 0.71$. Substituting these two values in equation (4.16) we get $M^2 = 0.73 M_{KK}^2 \frac{n}{2}$, in exact agreement with a best-fit of the points in figure 4a.

Recall from section 2 that for nonvanishing quark mass we found that there are two possible values of the quark condensate, differing in sign, but that only the negative condensate is stable. In section 3.2 the positive-condensate solution was explicitly shown to be unstable by showing that the pseudo-Goldstone mode Y was tachyonic for this configuration. Since

the field-theoretic arguments establishing the G M O R relation apply regardless of the sign of the quark condensate, the squared mass of this mode should also obey the G M O R relation, at least approximately, with an appropriate sign change. Recall that eq. (1.2) represents the first term in an expansion around $m_q = 0$. Now in the string description at $m_q = 0$, the D 6-brane configurations for positive and negative c are identical, except for a rotation of by π . Hence up to a crucial sign, the numerical coefficients in eq. (4.16) are unchanged and hence the tachyonic mode should satisfy $M_Y^2 \approx 0.73 M_{KK}^2 r_1$. From Figure 5, it does indeed appear that the slopes of the lowest-lying Y and Y' modes are equal, but opposite in sign. More precisely, our best-fit of the numerical results for negative c gave $M_Y^2 \approx 0.72 M_{KK}^2 r_1$, which gives agreement to within about 1.4%.

5. Multiple flavours ($N_f > 1$) and a holographic Vafa-Witten theorem

Consider a vector-like gauge theory with vanishing β -angle (like QCD) and N_f flavours, allowing identical mass $m_q > 0$. The Vafa-Witten theorem states that the vector-like $U(N_f)$ flavour symmetry cannot be spontaneously broken [14]. This theorem does not exclude the possibility that, at $m_q = 0$, the $U(N_f)$ -preserving vacuum becomes degenerate with one or more $U(N_f)$ -breaking vacua. In this section we discuss the holographic realization of the Vafa-Witten theorem, within the approximations implied by the validity of the supergravity/Born-Infeld theory. In particular, we are considering $N_c \neq 1$ and $N_f \neq N_c$. Note that, strictly speaking, the Vafa-Witten theorem need not apply to the gauge theory on the D4/D6-brane system because of the presence of Yukawa-like couplings between the fundamental fermions and the adjoint scalars. However, the latter scalar fields are massive and the theorem should certainly apply in a limit where the scalar masses are sent to infinity. Further, one expects the same result for large but finite masses since the vacuum should still not be sensitive to the scalars. In the present case, the scalar masses are likely of order $M_{KK} \approx M_{QCD}$ and so these couplings would not be suppressed. Hence from the gauge theory viewpoint, it is therefore not clear, *a priori*, whether the effect of these fields can change the vacuum structure of the theory to the extent of violating the Vafa-Witten theorem.¹¹ However, the results of this section answer this question in the negative.

The $U(N_f)$ global symmetry of the gauge theory corresponds, in the string description, to the $U(N_f)$ gauge symmetry on the worldvolume of N_f D6-brane probes in the geometry (2.1). Their dynamics is described by the so-called non-Abelian Dirac-Born-Infeld action [18]. This is a generalisation of the single-brane Abelian theory (2.16), in which both the gauge fields and the transverse scalars are promoted to Hermitian, $U(N_f)$ matrices. This means, in particular, that the positions of the D6-branes are no longer commuting quantities in general. In the particular cases in which the transverse scalar matrices can be simultaneously diagonalised, each of their N_f eigenvalues can be interpreted as the position of one of the D6-branes along the corresponding transverse direction.

¹¹We thank A. Nelson for a discussion on this point.

For the $U(N_f)$ global symmetry to be realized in the gauge theory, the mass matrix for the fundamental quarks must be diagonal with all eigenvalues equal to m_q . In our string picture, this translates into the boundary condition that, asymptotically, all the D 6-branes should have the same asymptotic boundary conditions. That is, they are all aligned with each other in the (z^5, \dots, z^9) subspace and all lie at a distance $2\sqrt{s}m_q$ from the origin. We would like to show that the configuration (which obviously satisfies the boundary condition above) in which all the D 6-branes are exactly coincident, and are embedded exactly as in the case of a single D 6-brane, is the minimum-energy solution of the equations of motion that follow from the non-Abelian DBI action.

To avoid problems with the coordinate singularity at $r = 0$, we adopt the Cartesian coordinates X and Y introduced in section 3.2 to describe the transverse positions of the D 6-branes in the r -plane. Then the configuration for the N_f coincident six-branes may be written as:

$$X(\tau) = r_{\text{vac}}(\tau) \mathbb{I}; \quad Y(\tau) = 0; \quad =_0 \mathbb{I}; \quad (5.1)$$

where $r_{\text{vac}}(\tau)$ is the profile for a single D 6-brane determined in section 2 and \mathbb{I} is the N_f N_f identity matrix. Since all the transverse scalars commute, there is no ambiguity in the interpretation of this solution as N_f overlapping D 6-branes lying along the curve $X(\tau) = r_{\text{vac}}(\tau)$.

Let us first argue that this configuration is a stable solution of the non-Abelian DBI equations of motion. We start by expanding the non-Abelian DBI action to quadratic order in fluctuations around the above configuration. Since there is an overall single trace in front of the action, to linear order only variations proportional to the identity generator couple to the $U(1)$ background fields, as given above. Hence the resulting expression for these fields is exactly that obtained from the linear variation of action for a single D 6-brane. It thus follows that the configuration (5.1) is a solution of the non-Abelian equations provided $r_{\text{vac}}(\tau)$ solves the corresponding Abelian equations.

We further observe that, to quadratic order in fluctuations, the non-Abelian DBI action reduces to the sum of N_f^2 identical copies of the Abelian action, one for each of the N_f^2 independent fluctuations. The reasons for this are two-fold: First, given that the background fields in (5.1) are proportional to the identity, the quadratic fluctuations must again contribute a term in the overall $U(1)$. Second, the difference between the non-Abelian and the Abelian DBI actions consists entirely of terms that involve commutators of fields. Hence, with the given background, the only possible nonvanishing commutators will involve two fluctuations, but such expressions are necessarily $SU(N_f)$ -valued, i.e., traceless. It follows that upon tracing over the gauge indices (and integrating by parts), the quadratic action will take the form

$$\frac{Z}{d^7} \sum_{i=1}^{N_f^2} Z^i O_{ij} Z^j; \quad (5.2)$$

where $Z^i = f X^i Y^g$, g is the colour index and O_{ij} is the same operator as appears in the quadratic expansion of the Abelian action. Thus the linearized equations of motion, and

hence the spectrum, are just N_f^2 copies of those in the Abelian theory describing a single D 6-brane embedding. It follows that the solution (5.1) is stable provided its Abelian analogue is stable, which we know to be the case from the analysis of section 3.

Note that these N_f^2 fluctuations of the D 6-branes, which give rise to the N_f^2 copies of the spectrum, are distinct physical excitations and not gauge-equivalent: each of them is associated to a different generator of $U(N_f)$, so there is no small $U(N_f)$ gauge transformation (that is, one that tends to the identity at infinity in the 0123-directions) that takes one mode into another. In particular, this implies that in the limit $m_q \rightarrow 0$ there are N_f^2 massless particles! We will come back to this point in the last section.

The arguments presented so far show that (5.1) provides a stable extremum of the non-Abelian DBI action, and therefore a local minimum of the energy of the N_f D 6-branes. Strictly speaking, this does not exclude the possibility that there exist other minima. If this was the case, then the true vacuum (or vacua) would be that (or those) with the lowest energy. On physical grounds, however, the existence of these other vacua is unlikely. The reason is as follows. If we ignore the interactions of the D 6-branes with each other, then it is clear that (5.1) is the minimum-energy solution amongst those satisfying the boundary conditions described above, since in the absence of interactions each D 6-brane must minimise its own energy. If we include open string tree-level interactions by describing the D 6-branes' dynamics with the non-Abelian DBI action, then the only obvious configuration that satisfies the appropriate boundary conditions is (5.1), which we have shown to be a stable solution. Inclusion of one-loop (or higher) open string interactions between the D 6-branes (such as exchange of closed strings) would presumably just strengthen the conclusion that (5.1) is the preferred solution. To see this, consider the simple case of $N_f = 2$ D 6-branes that overlap with each other asymptotically, but that are slightly misaligned in some small region. Locally, this situation is analogous to that of two planar D 6-branes in flat space that are almost but not exactly parallel, in which we know that there is a net force that tends to align the branes. It seems plausible that a similar force will act on the branes in the situation of interest here, and therefore that the preferred configuration will be (5.1), in which all the branes are perfectly aligned with each other.

This conclusion provides a holographic realization of the Vafa-Witten theorem, since the $U(N_f)$ gauge symmetry on the D 6-branes is unbroken if and only if they are all exactly coincident.

By continuity, the arguments above imply that, in the limit $m_q \rightarrow 0$, the $U(N_f)$ -preserving configuration has an energy no greater than that of any other configuration. Just like in the Vafa-Witten theorem, however, this does not rule out the possibility that in this limit some other state becomes degenerate with that in eq. (5.1). In fact, the appearance of N_f^2 massless modes in the linearized spectrum at $m_q = 0$ suggests that the D 6-branes might be free to rotate independently in the 89-plane.¹² To see that this is indeed the case, consider, for

¹²Note that this is not guaranteed by the existence of massless modes, since this does not exclude the appearance of higher order potential terms for the fluctuations, e.g. z^4 .

simplicity, the $N_f = 2$ configuration

$$X(\phi) = r_{\text{vac}}(\phi) \cos \phi_0 \mathbb{I}; \quad Y(\phi) = r_{\text{vac}}(\phi) \sin \phi_0 \mathbb{I}; \quad =_0 \mathbb{I}; \quad (5.3)$$

where $\mathbb{I}_3 = \text{diag}(1; 1; 1)$ and ϕ_0 is some fixed angle. The radial vacuum profile above is that corresponding to $r_1 = 0$. This configuration consists of two D6-branes with the same radial profiles but separated an angle $2\phi_0$ in the 89 -plane, and obviously satisfies the boundary condition that the branes overlap at $\phi = 0$. To see that it solves the non-Abelian equations of motion, consider expanding the non-Abelian DBI action to linear order in fluctuations around (5.3), as before. Since commutator terms are irrelevant at this order, and X and Y are diagonal, the non-Abelian action again reduces to the sum of two identical Abelian actions. In fact, the same argument shows that not only is the configuration (5.3) a solution of the non-Abelian equations, but also that its energy is, for all ϕ_0 , equal to twice that of a single D6-brane. It follows that (5.3) is stable for all ϕ_0 . To see this, suppose that it is not, i.e., that there is some fluctuation around it that is tachyonic. Presumably, this would mean that this solution can decay to another one of lower energy. However, the latter would also have lower energy than the solution with $\phi_0 = 0$, in contradiction with our continuity argument above.

Note that the previous reasoning applies equally well to any distribution of N_f D6-branes around the ϕ -circle, since it only relies on X and Y being diagonal. Thus, at $m_q = 0$, all these configurations are degenerate, lowest-energy, stable solutions. Although it may be an interesting exercise to verify their stability explicitly by expanding the non-Abelian DBI action to quadratic order in fluctuations around (5.3), one should keep in mind that this conclusion is only expected to hold at leading order in the $1=N_f$ expansion, since, as discussed above, we expect higher-order effects to lead to an attractive force between the branes, which would tend to align them.

6. Finite Temperature Physics

The gauge theory we have so far been describing is at zero temperature. To study the theory at a finite temperature T , we may follow the standard prescription: analytically continue the time coordinate $t \rightarrow t_E = it$, periodically identify t_E with period $t_E = 1/T$, and impose anti-periodic boundary conditions on the fermions around the t_E -circle. This prescription applies equally well in the gauge theory and in the dual string description. In the latter, however, one must consider all possible spacetime solutions with the appropriate boundary conditions, that is, possible saddle points Euclidean path integral over supergravity (or rather, string) configurations [2].

In the present case, there are two¹³ Euclidean supergravity solutions which must be

¹³In analogy with [19], there may be an infinite family of Euclidean solutions labelled by two integers specifying which cycle of the t_E -torus shrinks to zero-size in the bulk. However, given that the t_E - and ϕ -axes are orthogonal, here either the solutions in eq. (6.1) or (6.2) will dominate the path integral.

considered. The first is simply the Euclideanised version of that appearing in eq. (2.1),

$$ds^2 = \frac{U}{R} \sum_{i=1}^{3=2} dt_E^2 + \frac{X^3}{R} dx^i dx^i + f(U) d^2 + \frac{R}{U} \frac{3=2}{f(U)} \frac{dU^2}{f(U)} + R^{3=2} U^{1=2} d^2; \quad (6.1)$$

which dominates at low temperatures. Recall that $f = 1 - U_{KK}^3 = U^3$. The second is the Euclidean black hole coming from a nonextremal 4-brane throat

$$ds^2 = \frac{U}{R} \sum_{i=1}^{3=2} f(U) dt_E^2 + \frac{X^3}{R} dx^i dx^i + d^2 + \frac{R}{U} \frac{3=2}{f(U)} \frac{dU^2}{f(U)} + R^{3=2} U^{1=2} d^2; \quad (6.2)$$

which dominates at high temperatures. In this case, $f = 1 - U_T^3 = U^3$. In the Lorentzian-signature solution, the event horizon is located at $U = U_T$.

Of course, these Euclidean metrics are identical up to interchanging the role of t_E and (and replacing U_{KK} with U_T). To match the boundary conditions set by the finite-temperature gauge theory, we identify these coordinates with periods

$$t_E = \frac{1}{T}; \quad = \frac{2}{M_{KK}}; \quad (6.3)$$

in both solutions. Since we wish to avoid conical singularities in either spacetime at $U = U_{KK}; U_T$, the boundary conditions x the metric parameters as

$$U_{KK} = \frac{4}{3} R^2; \quad U_T = \frac{4}{3} \frac{2}{t_E} R^2; \quad (6.4)$$

As we commented above, the metric (6.1) dominates the path integral at low temperatures, whereas that given by eq. (6.2) dominates at high temperatures. One determines the transition point by comparing the Euclidean action of these two solutions [2]. As the metrics describe the same geometry, it is easy to see that the transition occurs precisely when $t_E = t$. That is, a phase transition occurs at the critical temperature

$$T_{deconf} = M_{KK} = 2; \quad (6.5)$$

From the gauge theory viewpoint, this is a confinement/deconfinement phase transition. This can be seen by the fact that the temporal Wilson loop (around t_E) vanishes for the low-temperature background (6.1), whereas it is nonvanishing for the Euclidean black hole (6.2) [2]. Alternatively, on the Lorentzian sections, the Wilson loop as computed from the solution (2.1) exhibits an area law behaviour, while that computed for the Lorentzian black hole does not because the string can break in two pieces, each having an endpoint at the horizon [21]. One might also observe that, in the low-temperature phase, one has a discrete spectrum of glueballs [3], but this gives way to a continuum of excitations in the high-temperature phase dual to the black hole background.¹⁴ The analogous phase transition in 3+1 dimensions was

¹⁴Note that the spectrum would again be calculated with Lorentzian signature.

discussed in ref. [20]. Finally, note that the phase transition takes place at a temperature, (6.5), where the gauge theory is starting to behave *ve-dimensionally*, rather than *four-dimensionally*.

The preceding discussion refers only to the physics of the (com pactified) *ve-dim*ensional gauge theory and is independent of the presence of fundamental matter fields. In previous sections we have exhaustively analysed the physics of dynamical quarks in the *confining* phase. We can extend the discussion to the *deconfining* phase by considering probe D 6-branes in the black hole background (6.2). In reference [9] the study of D 7-branes in an asymptotically AdS₅ black hole background revealed the existence of two sets of regular embeddings, parametrised by the quark mass and chiral condensate of the dual gauge theory, and distinguished by whether or not the D 7-brane intersects the horizon. It was suggested that the gauge theory undergoes a phase transition, signalled by a discontinuity in $dc=dm_q$, when the D 7-brane undergoes its 'geometric' transition. Here we consider similar physics in our four-dimensional gauge theory.

As before, the D 6-branes span (Euclidean) time and the spatial 123-directions in common with the D 4-brane worldvolume, and lie at a fixed value of τ . In parallel with the steps described by eqs. (2.11)-(2.14), we introduce isotropic coordinates f_1, f_2, r, θ for the Euclidean black hole (6.2). Furthermore, we rescale to dimensionless coordinates

$$! U_T ; \quad r ! U_T r ; \quad ! U_T ; \quad (6.6)$$

in analogy with eq. (2.18). Now the embedding equation for $r(\tau)$ becomes

$$\frac{d}{d\tau} \left(\frac{1}{4} \frac{r^2}{1+r^2} \right)^2 = \frac{3}{8} \frac{r^2 p}{1+r^2} \frac{r}{1+r^2} ; \quad (6.7)$$

Comparing this result with eq. (2.19), we see that the sign of the right-hand side has changed. As we will see below, this change of sign indicates that the brane now bends towards $U = U_T$: as expected, the black hole exerts an attractive force on the D 6-brane, in contrast to the repulsive force in the D 4-soliton background.

If we look for asymptotically constant embeddings such that $r(\tau) \rightarrow r_1 = L = U_T$ as $\tau \rightarrow 1$, we find the same long-distance behaviour as before:

$$r' \rightarrow r_1 + \frac{C}{\tau} ; \quad (6.8)$$

These asymptotic parameters are related to the quark mass and chiral condensate as before, except for the substitution of U_T for U_{KK} :

$$m_q = \frac{U_T r_1}{2 \sqrt{s}} ; \quad h \quad i = 8 \sqrt{s} T_{D6} U_T^2 C ; \quad (6.9)$$

Again, the embedding equation can be solved numerically for any value of r_1 , with the asymptotic boundary conditions implicit in (6.8). Inspection of the results reveals that, just as in reference [9], two qualitatively different types of profile are possible: those for which

the probe brane intersects the horizon, and those for which it does not. As we vary the boundary condition r_1 , we find that there is a unique embedding for sufficiently large or small values. In the case of small r_1 , the unique embedding is such that the D 6-brane falls into the horizon, whereas in the large- r_1 case it does not, despite, of course, still being attracted by the black hole. For an intermediate range with $r_1 > 1$, we find that more than one embedding is possible. In particular, for a given r_1 , we find both embeddings which intersect the horizon and those where the D 6-brane smoothly closes off before reaching the horizon. Furthermore, we also find that there are typically multiple solutions of at least one of these varieties of embedding; figure 6 displays some representative examples. These results imply that in varying from large to small r_1 , there will be a phase transition in the behaviour of the quarks. This transition will occur in the intermediate regime, where, for a fixed temperature and quark mass, the condensate in the gauge theory can have multiple values. Of course, the true ground-state condensate will be selected by minimizing the energy density.

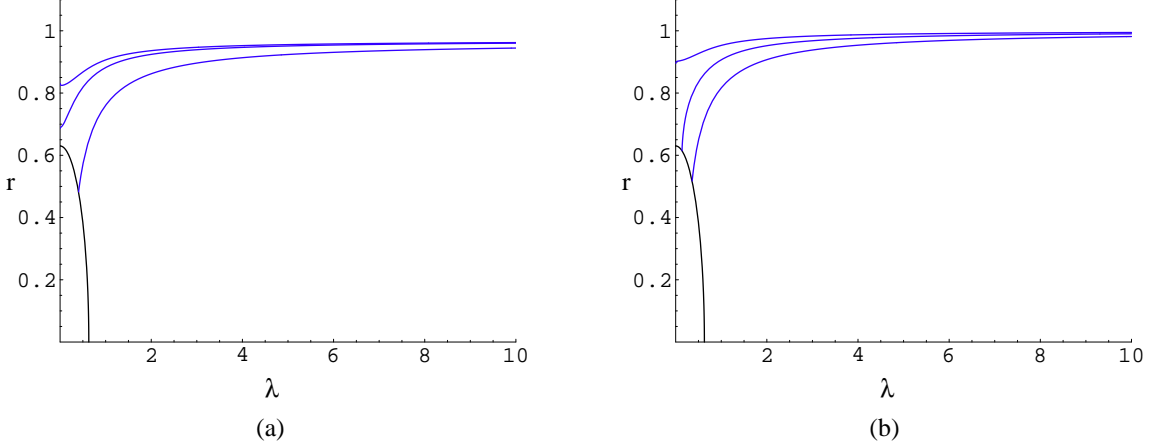


Figure 6: Some representative D 6-brane embeddings from the region in which c is multi-valued. The three profiles in each figure have the same asymptotic value of r_1 ; in (a) two of them avoid the horizon whereas in (b) two fall into the horizon.

Combining various results [see eqs. (2.6), (6.3), (6.4) and (6.9)] the relation between the temperature and r_1 is found to be

$$T = \frac{M}{p \frac{r_1}{r_1}} ; \quad \text{with } M^2 = \frac{9}{4} \frac{m_q M_{KK}}{g_{YM}^2 N_c} ; \quad (6.10)$$

Here M can be interpreted, for a given quark mass, as the typical meson mass scale in the regime where supersymmetry is restored in the zero-temperature gauge theory [see the discussion below eq. (3.16)]. In the zero-temperature analysis of previous sections we regarded the variation of r_1 as a variation of the quark mass, while U_{KK} or, equivalently, the KK scale, was fixed. In this section we wish to study the phase structure of the gauge theory as the temperature is varied, keeping the microscopic gauge theory parameters, and in particular

the quark mass, m is fixed. For this reason, since in this phase the physics will only depend on the ratio T/M , as suggested by eq. (6.10), we will think of the variation of r_1 as a variation of the temperature.

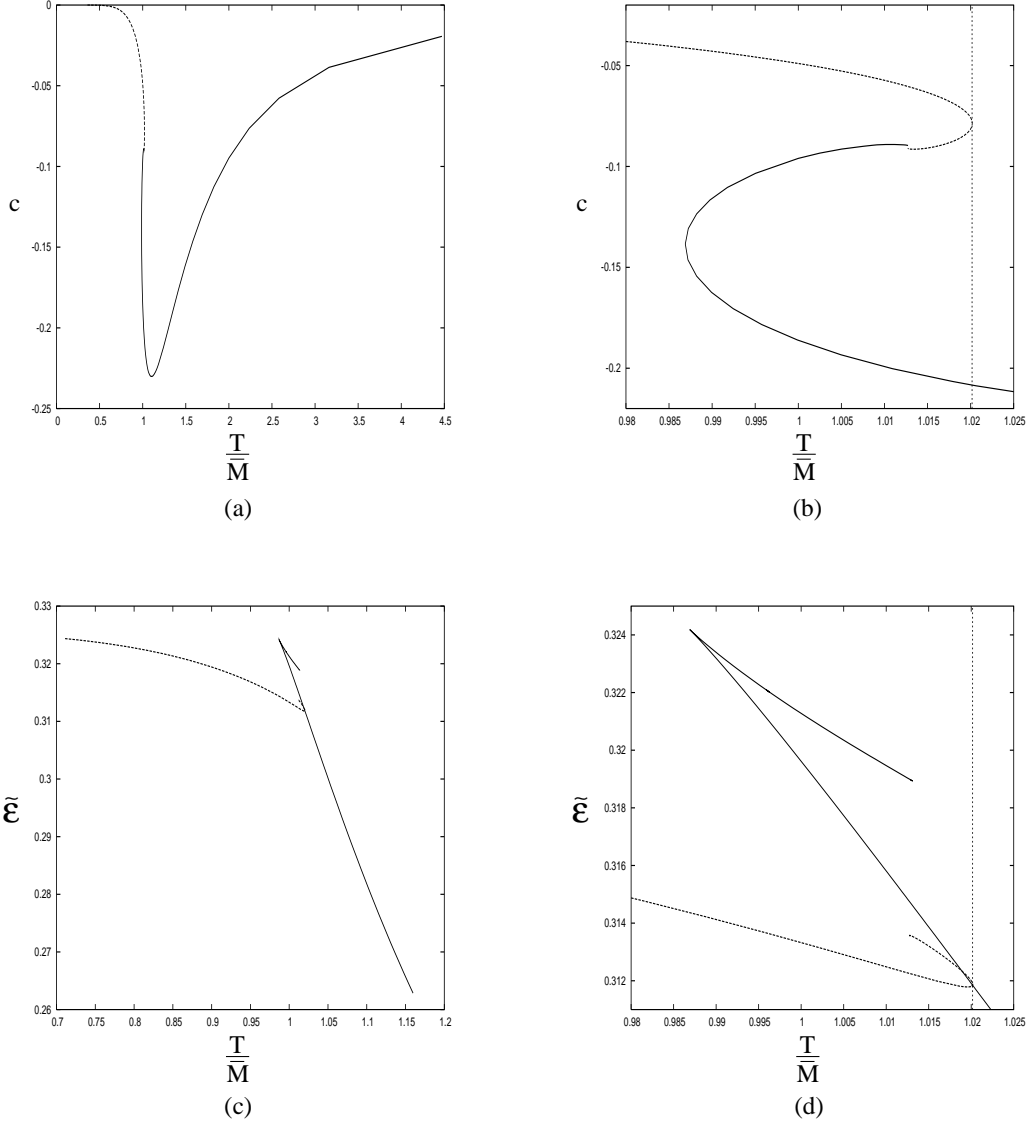


Figure 7: The quark condensate $h \bar{c} / c$ (plots (a) and (b)), and the energy density $E \bar{c}$ (plots (c) and (d)) as functions of temperature. The solid (dashed) lines describe the family of embeddings that do (not) intersect the horizon. Plots (b) and (d) show in more detail the regions of plots (a) and (c) where the two branches intersect. The vertical line lies at $T = T_{\text{bind}}$, the temperature at which the phase transition in the behaviour of the quarks takes place.

The behaviour of the condensate (represented by c) as a function of the temperature is shown in figures 7a and 7b. These plots display some interesting features. First note that $c \rightarrow 0$ both as $T \rightarrow 0$ and as $T \rightarrow 1$. In the high-temperature regime, the unique embedding

is such that the D 6-brane falls into the horizon. By following the solid line in the figure, we see that these embeddings only exist down to some minimum temperature, $T' = 0.9869M$. Similarly there is a unique embedding at sufficiently low temperatures such that the D 6-brane does not reach the horizon, and following the dashed line shows that embeddings of this form only exist up to $T' = 1.0202M$. As shown most clearly in figure 7b, multiple solutions exist in the intermediate temperature range between the two values given above.

Naturally, where more than one solution to the embedding equation exists, the ground-state profile will be that selected out by lowest energy density. Since we are considering static configurations, the energy density is given by

$$E = \int d^d r \frac{1}{2} L = \frac{1}{4} T_{D6} U_T^3 \int_{r_{\text{in}}}^{r_{\text{out}}} dr \frac{1}{2} \left(\frac{1}{4^3} \right)^2 \frac{r^2}{1+r^2} ; \quad (6.11)$$

where r_{in} is either zero, or the point where the brane meets the horizon, depending on which variety of embedding we are considering. This integral is divergent, so to compare the energy densities of different embeddings we regularize E by using as a reference the embedding $r(r) = 0$, which runs from the horizon (at $r = r_H$, say) to infinity. Since this is a numerical calculation, we also introduce a cut-off, r_{match} , in r at the point where, by imposing the appropriate boundary conditions, we match the numerical profile to the asymptotic solution, $r' = r_1 + c$. There is an infinite contribution to E from the remainder of the profile, but when regularized the leading behaviour of this correction can be shown to be

$$E_{\text{corr}} = \frac{c^2}{2 r_{\text{match}}} + O\left(\frac{1}{r_{\text{match}}^3}\right) ; \quad (6.12)$$

Therefore, to be precise, we compare the energy densities by calculating

$$E = \frac{E_{\text{reg}}}{4 T_{D6} U_T^3} \int_{r_{\text{in}}}^{r_{\text{match}}} dr \frac{1}{2} \left(\frac{1}{4^3} \right)^2 \frac{r^2}{1+r^2} + \int_{r_H}^{r_{\text{match}}} dr \frac{1}{2} \left(\frac{1}{16^4} \right) + \frac{c^2}{2 r_{\text{match}}} ; \quad (6.13)$$

We then trust that this provides a valid basis for the comparison of different energy densities when the differences in E are greater than $O\left(\frac{1}{r_{\text{match}}^3}\right)$. This is the case here, as we use $r_{\text{match}} = 100$.

The energy density E is plotted as a function of temperature in figures 7c and 7d. Starting from low temperatures, figure 7d shows that, as T is increased to that in the intermediate region, the physical embedding remains that which does not reach the horizon. At $T' = 1.0202M$, the energy density for this embedding and that which falls into the horizon match. For $T > 1.0202M$, the energetically favoured embedding is one which falls into the horizon. Therefore, at

$$T = T_{\text{fund}} = 1.0202M ; \quad (6.14)$$

there is a phase transition in the behaviour of the fundamental quarks. This phase transition is signalled by a discontinuity in $h = h(T)$, as shown in Figure 7b, as well as a discontinuity in

the specific heat $dE(T)/dT$, as can be seen in Figure 7d. Note that, to within the precision of our numerical calculations, T_{fund} cannot be distinguished from the maximum temperature for which a horizon-avoiding embedding is possible.

From the string description with the D 4 throat geometry, the basic physics behind this transition is straightforward. Increasing the temperature increases both the radial position of the horizon and energy density of the black hole. For small enough a temperature, the D 6-brane is pulled towards the horizon but its tension balances the gravitational attraction. However, above the critical temperature T_{fund} , the gravitational force has increased to the point where it overcomes the tension and the brane is drawn into the horizon.

Another feature that characterizes the present phase transition is that the meson spectrum changes at $T = T_{\text{fund}}$. The discrete spectrum of mesons of the low-temperature phase becomes a continuum of excitations in the high-temperature phase where the D 6-brane embedding extends to the horizon. This behaviour is similar to that of the glueball spectrum at the deconfinement phase transition in the gauge theory, discussed previously. Note, however, that for temperatures above T_{deconf} we are, by assumption, in the deconfined phase of the gauge theory, and so it is possible to introduce free quarks; these correspond to open strings extending from the D 6-brane down to the horizon. If $T_{\text{deconf}} < T_{\text{fund}}$ there is then a range of temperatures, $T_{\text{deconf}} < T < T_{\text{fund}}$, in which there are free quarks but also a finite mass gap, $m_e(T) > 0$, associated with the introduction of such quarks into the system. In this regime, there still exists a (discrete) spectrum of bound states with $M < 2m_e$. Note also that the deconfined adjoint degrees of freedom still generate a finite screening length beyond which the force between a quark and an anti-quark vanishes [21]; in the string description this happens because the string that joins the quarks together snaps into two pieces, each of them going from the brane to the horizon, that can be separated with no cost in energy. Above T_{fund} , however, $m_e(T) = 0$ and the spectrum of fundamental matter field excitations becomes continuous.

Up to this point, we have discussed two independent phase transitions: the deconfining phase transition at $T = T_{\text{deconf}}$, for which the holographic dual description involved a discrete change of the bulk spacetime geometry, and the quark phase transition at $T = T_{\text{fund}}$, for which the holographic description involved a discrete jump in the embedding geometry of the D 6-brane. However, if the latter is to be realized as a separate phase transition, then it must be true that $T_{\text{fund}} > T_{\text{deconf}}$.¹⁵ In terms of the microscopic parameters, this condition translates into

$$m_q > \frac{0.98}{9} g_{YM}^2 N_c M_{KK} : \quad (6.15)$$

In the zero-temperature theory, this is roughly the quark mass scale at which supersymmetry is restored | see the discussion below eq. (3.16).

¹⁵ Note that, in this regime, the fundamental fields still 'feel' the deconfining transition at $T = T_{\text{deconf}}$. For example, there is a discontinuity in the chiral condensate h_{ii} , which jumps from a negative to a positive value at this phase transition.

If $T_{\text{fund}} < T_{\text{deconf}}$, the relevant spacetime geometry at $T = T_{\text{fund}}$ is the D 4-soliton (6.1) and the ambiguity in the D 6-brane embedding discussed above is not relevant. Alternatively, the gauge theory is still in a confined phase and so the chemical potential to introduce a free quark remains finite; in the dual description this is because, since there is no horizon, an open string must have both ends on the D 6-brane, and so represents a quark/anti-quark bound state. In this case, the two phase transitions are realized simultaneously at $T = T_{\text{deconf}}$. An important example of this behaviour is when $m_q = 0$. In this case, the low-temperature phase is characterized by spontaneous chiral symmetry breaking, as in section 2. In the high-temperature phase, $m_q \neq 0$ is equivalent to $T \neq 1$ (see eq. (6.10)), in which limit the chiral condensate vanishes (see figure 7a). Hence the deconfining phase transition is also accompanied by the restoration of chiral symmetry in this model.

To close the section, we wish to stress to the reader that while these phase transitions are of inherent interest in understanding the model under study here, they take place in a temperature regime where the gauge theory is intrinsically $2+1$ -dimensional, rather than behaving in a four-dimensional way, as can be seen by comparing the transition temperatures given in eqs. (6.5) and (6.15) to the compactification scale M_{KK} .

7. D 4/D 6/ $\overline{\text{D} 6}$ -intersections

In the discussion of embeddings in section 2, we noted that the solution $r(\phi) = 0$ of eq. (2.19) is not a physical one (for $U_{KK} \neq 0$) if it terminates at the origin of the U -plane because it would correspond to an open D 6-brane. However, this solution can be extended through this point to construct a physically acceptable embedding. To see this, recall that the full D 6-brane embedding is further specified by the conditions $\phi = 0$ and $\dot{\phi} = 0$, where 0 and $\dot{0}$ are arbitrary constants. We can therefore join together a solution with $\phi = 0$ to another one with $\phi = 0 + \phi = 2$ (see eq. (2.3)) to obtain a complete regular solution that describes a D 6-brane whose projection on the U -plane is a straight line that passes through the origin and intersects the boundary at two antipodal values of ϕ . This means that this solution describes an intersection of N D 4-branes with two D 6-branes, or, more precisely, with one D 6-brane and one anti-D 6-brane.¹⁶

To better understand the defect theory corresponding to these D 4/D 6/ $\overline{\text{D} 6}$ -intersections, we consider a family of more general embeddings that describe D 6-branes that lie at $r = 0$ (or alternatively, $z^8 = 0 = z^9$) and stretch along some curve $U = U(\phi)$ in the U -plane, intersecting the boundary at two, not necessarily antipodal, values of ϕ . Such D 6-branes wrap a maximal S^2 within the S^4 in the metric (2.1), so the induced metric on their worldvolume is

$$ds^2(g) = \frac{U}{R}^{3=2} dx^3 dx^2 + R^{3=2} U^{1=2} d\phi^2 + \frac{U}{R}^{3=2} f(U) + \frac{U^{2=2}}{\frac{U}{R}^{3=2} f(U)} d\theta^2 : (7.1)$$

¹⁶Technically, the reason is that the orientations on the intersections of the D 6-brane with the boundary at $\phi = 0$ and $\phi = 0 + \phi = 2$, induced from a given orientation on the D 6-brane, are opposite to each other.

Since the Lagrangian density on the D 6-brane

$$L_{D6} = \frac{1}{(2\pi)^6 \sqrt{s}} e^{-p \frac{s}{\det g_{\text{d}}}} = T_{D6} U^2 \frac{\frac{U}{R}^3}{f(U)} + \frac{\frac{U}{R}^2}{f(U)} \quad (7.2)$$

(where $U^0 = dU = d$) does not depend explicitly on U^0 , it follows that

$$U^0 \frac{\partial L}{\partial U^0} = L = \frac{U^2 \frac{U}{R}^3 f(U)}{\frac{U}{R}^3 f(U) + \frac{U}{R}^2} \quad (7.3)$$

is also U^0 -independent. Let $U_0 = U_{KK}$ be the minimum value of $U(U)$. By symmetry we can assume that this value is reached at $U^0 = 0$, that is, that we have $U(0) = U_0$ and $U^0(0) = 0$. Integrating the equation above we then find

$$\sim(u) = \frac{3}{2} b^{7/2} g^{1/2}(b) \int_b^u \frac{dx}{x^{3/2} g(x)} = \frac{1}{b^{1/2} g(b)}; \quad (7.4)$$

where we have introduced

$$\sim(u) = \frac{3}{2} \frac{U_{KK}^{1/2}}{R^{3/2}}; \quad u = \frac{U}{U_{KK}}; \quad b = \frac{U_0}{U_{KK}} = 1; \quad g(x) = 1 - \frac{1}{x^3}; \quad (7.5)$$

Note that the rescaled angle $\sim(u)$ has period 2. Eq. (7.4) specifies the D 6-brane profile in the U^0 -plane. The D 6-brane intersects the boundary at $\sim(b) = \sim(u) = 1$. These two points are implicitly fixed by U_0 , the 'lowest' point of the D 6-brane in the U^0 -plane. In particular, their separation is a monotonically decreasing function of b . It is easy to show that $\sim(b = 1) = \sim(u = 1) = 2$, so the two points become antipodal as the lowest point of the D 6-brane approaches the origin of the U^0 -plane. In this limit the projection of the D 6-brane on this plane is just a straight line, as discussed above. In the opposite limit in which the (lowest point of) D 6-brane approaches the boundary, the separation between the intersection points becomes smaller and smaller. In the strict limit $b = 1$ the two coincide and the D 6-brane disappears.

Now, these embeddings seem to portend fascinating physics for the dual 6 -dimensional gauge theory coupled to two defects or, more precisely, to a defect and an anti-defect. It appears, however, that this physics is intrinsically 6 -dimensional. Since the focus of the present paper is the four-dimensional QCD-like physics of the original model, we have not fully explored this system. However, we offer some preliminary remarks in the following.

The direction of the D 6-brane in the U^0 -direction, which corresponds to a worldvolume direction of the D 4-branes, is reminiscent of certain D 5-brane embeddings in AdS₅ studied in ref. [22]. These authors found (non-supersymmetric) embeddings in which the D 5-brane began at large radius running along r , but were deformed to run parallel to the AdS₅ horizon at some finite radius. At large r , these configurations can be understood as D 3/D 5 intersections that are T-dual to that represented in (1.1). The dual gauge theory involved coupling $N = 4$

SYM to a $(2+1)$ -dimensional defect which broke all supersymmetries. The detection was interpreted as giving an expectation value to an operator in the defect theory.

In the present case, the D 4-soliton background breaks the supersymmetry but with both defects, supersymmetry would still not be restored in the limit $U_{KK} \rightarrow 0$.¹⁷ One way to understand this in the field theory is to note that the half of the supersymmetries of the ambient theory preserved (broken) by the defect are precisely those that are broken (preserved) by the anti-defect.¹⁸ The embeddings described by eq. (7.4) would correspond to a state where a symmetric pair of operators in each defect theory simultaneously acquire identical expectation values. Indirectly, the D 6-brane embedding would also induce different expectation values of gauge theory operators, e.g., $\text{Tr } F^2$, in the two regions on the \mathbb{R} -circle divided by the defects.

At the microscopic level, there are two sets of fundamental matter fields in the field theory, one associated with each defect. This is realised in the string description by the fact that, despite there being a single D 6-brane, its intersection with a constant $U > U_0$ slice consists of two disconnected pieces, corresponding to two independent sets of active degrees of freedom at the corresponding energy scale. These degrees of freedom seem to disappear for energy scales associated to radial positions $U < U_0$, as in [22]. As discussed above, the D 6-brane disappears in the limit $\sim \sim \rightarrow 0$. Consistently, in this limit $U_0 \rightarrow 1$ and the degrees of freedom above are completely removed. In the gauge theory, this corresponds to the limit in which the defect and the anti-defect are brought on top of each other.

This situation may be compared with that where both defects are associated with a ‘standard’ D 6-brane embedding as described in section 2; one at $\sim = \gamma$ and the other at $\sim = \gamma$. Of course, in this case there are also two sets of independent degrees of freedom associated with open string excitations on both the D 6- and $\overline{\text{D}6}$ -brane.¹⁹ However, one difference is that the spectrum of these excitations will now be independent of the defect/anti-defect separation, $\sim \sim$.²⁰ In addition, one would also find excitations corresponding to open strings stretching between the two separate branes. In contrast, in the case of a single D 6-brane, the two defects can interact through open string modes that propagate along the brane from one defect to the other.

Of course, one should ask the question which embedding minimizes the energy density of the system. That is, does energetics favour the smooth embedding which joins the two boundary defects or that in which there are two independent branes? Note, however, that the above are just two particular cases of a more general family of embeddings in which the brane bends simultaneously in the 89 - and the U -planes, that is, embeddings of the form $U = U(\gamma)$. The minimal energy two-defect embedding is presumably of this type.

¹⁷Note that the supersymmetry breaking of the background is not essential to constructing the general embeddings, i.e., one can simply replace $g(x)$ by 1 everywhere in eq. (7.4).

¹⁸Defect/anti-defect configurations, and more general multiple defect configurations, were discussed in [23].

¹⁹Note that in this case one may also realise a defect/defect (as opposed to a defect/anti-defect) theory by considering two D 6-branes.

²⁰In the approximation in which interactions between the branes, which are suppressed in the large- N limit, are neglected.

8. Discussion

We have analyzed in detail the case of a single D 6-brane, which corresponds to a single flavour in the gauge theory. In this case the gauge theory enjoys (at large N_c) an exact $U(1)_V \times U(1)_A$ symmetry. The first factor is just the flavour symmetry, which in the string description corresponds to the gauge symmetry on the worldvolume of the D 6-brane. The second factor is a chiral symmetry that rotates the left- and right-handed fermions, ψ_L and ψ_R , with opposite phases; it also rotates by a phase the adjoint scalar $X = X^8 + iX^9$, as is clear from the fact that in the string description the $U(1)_A$ symmetry is just the rotational symmetry in the 89 -plane.

Like in QCD, we expect the $U(1)_A$ symmetry to be spontaneously broken by a chiral condensate, $h \neq 0$, and hence the existence of the corresponding Goldstone boson in the spectrum; this is the analog of the QCD π^0 particle (which is massless in the $N_c \rightarrow 1$ limit), but, in an abuse of language, we have referred to it as a 'pion'. The string description indeed confirms the field theory expectation: for zero quark mass, there is precisely one massless (in the four-dimensional sense) fluctuation of the D 6-brane. If $m_q > 0$ this pion becomes a pseudo-Goldstone boson. Its mass, as well as the chiral condensate and the pion decay constant, can be computed in the string description, and we have shown that these three quantities and the quark mass obey the Gell-Mann-Oakes-Renner relation (1.2) [13]. Although this is a reassuring result, one should keep in mind that, just like in field theory, it is essentially a consequence of the symmetry-breaking pattern.

In the case $N_f > 1$ we provided a holographic version of the Vafa-Witten theorem, which states that, in a vector-like theory with zero -angle (like QCD) and N_f quark flavours of identical masses $m_q > 0$, the global, $U(N_f)$ flavour symmetry cannot be spontaneously broken. As we discussed, it is a priori unclear, on field theory grounds, that the Vafa-Witten theorem does apply to the actual gauge theory on the D 4-branes, because of the presence of Yukawa-like couplings to scalar fields of masses $M_{KK} \ll M_{QCD}$. The result from the string analysis therefore established that the presence of these fields does not alter the vacuum structure of the theory to the extent of violating the Vafa-Witten theorem.

The global $U(N_f)$ symmetry of the gauge theory becomes the gauge symmetry on the worldvolume of N_f D 6-branes in the string description. The holographic version of the Vafa-Witten theorem is the statement that the minimum energy configuration for the N_f D 6-branes is a $U(N_f)$ -preserving one in which all branes lie on top of each other. It should be emphasised that, unlike the Gell-Mann-Oakes-Renner relation, the Vafa-Witten theorem is not based on a symmetry (breaking) argument, but depends on the dynamics of the theory. In the field theory, the proof relies on the reality and positivity of the fermion determinant that arises in the path integral formulation; in the holographic version, it relies on details of the dynamics of multiple D 6-branes.

One result of our analysis of the $N_f > 1$ case is the existence of N_f^2 independent, massless fluctuations of the D 6-branes if $m_q = 0$. It is tempting to interpret the associated N_f^2 massless scalar particles in the spectrum of the gauge theory as the Goldstone bosons of a spontaneously

broken $U(N_f)_A$ symmetry, to which the $U(1)_A$ symmetry would putatively be enhanced for $N_f > 1$. However, only one of the N_f^2 states above is a true Goldstone boson, for two reasons. First, the 7 -dimensional theory contains a term of the form $i X^i$, where $i = 1, \dots, N_f$ is the flavor index. Since X^i only transforms under the $U(1)_A$ subgroup of $U(N_f)_A$, the theory is only invariant under $U(1)_A \times U(N_f)_V$, which is spontaneously broken to $U(N_f)_V$. Although X^i is a massive field that can be integrated out, its mass $M_X \sim M_{KK} \sim M_{QCD}$ is of the same order as the strong coupling scale, so its integration does not lead to a real suppression of the symmetry-breaking operator above.

The second reason that makes it plausible the interpretation of all but one of the massless modes above as Goldstone bosons is that they have non-derivative interactions. Indeed, the effective, interacting Lagrangian for these modes is obtained by expanding the non-Abelian Dirac-Born-Infeld action for the N_f D6-branes [18] beyond quadratic order and then dimensionally reducing it to four dimensions, as we did in Section 4 in the $N_f = 1$ case. Since the action for the D6-branes contains non-derivative interactions, such as commutator terms squared, so does the effective four-dimensional Lagrangian. These terms are only absent for the mode that multiplies the identity generator of $U(N_f)$. The caveat as to why this argument makes the Goldstone boson interpretation for the other modes plausible, but not strictly impossible, is that the coefficients in the effective Lagrangian might conspire so that, once all contributing diagrams are included, only momentum-dependent parts survive in any scattering amplitude (as in the linear sigma model for the pion Lagrangian [24]). This possibility seems rather unlikely.

Thus we conclude that the string description predicts the existence of $N_f^2 - 1$ massless scalar particles in the spectrum of the quantum gauge theory in the large- N_c limit. Once sub-leading effects in the $1/N_c$ expansion are included, we expect these particles to acquire a small mass. The $U(1)_A$ symmetry is anomalous at finite N_c , so its associated Goldstone boson is not exactly massless at finite N_c ; presumably, this anomaly can be analysed in the supergravity description along the lines of [25]. The other $N_f^2 - 1$ modes are likely to acquire a mass due to closed string interactions between the D6-branes, which are a $g_s = 1/N_c$ effect. From the gauge theory viewpoint there is no obvious reason for the masslessness (or lightness, at finite N_c) of these $N_f^2 - 1$ scalars, since we have argued that they are not Goldstone bosons.²¹ Recall that, from the string viewpoint, the reason for this is that the only difference between the non-Abelian and the Abelian DBI actions consists exclusively of terms that involve commutators of fields. This can be regarded as a consequence of the fact that the seven-dimensional D6-brane action is T-dual to the ten-dimensional action of D9-branes; all commutators of scalar fields in the D6-brane action originate from commutators of gauge fields in the non-Abelian field strength on the D9-branes. Thus, it is ten-dimensional $U(N_f)$ gauge invariance that seems to be responsible, from the string viewpoint, for the lightness of the gauge theory scalars.²² Given the importance in high energy physics of mechanisms that naturally allow small scalar

²¹Other examples with ‘unexpectedly’ light scalars in the context of AdS/CFT have been discussed in [26].

²²This observation is due to M. Strassler.

masses, it would be interesting to understand how to rephrase the constraints imposed by ten-dimensional $U(N_f)$ gauge invariance purely in four-dimensional field theory terms.

Acknowledgments

We are especially grateful to J. Brodie for helpful conversations. We also wish to thank J. Donoghue, J. Erdmenger, J. I. Latorre, A. E. Nelson, D. T. Son, M. J. Strassler, S. Thomas and D. Tong for discussions and comments. Research at the Perimeter Institute is supported in part by funds from NSERC of Canada. RCM is further supported by an NSERC Discovery grant, D JW by Fonds FCAR du Québec and by a McGill Major Fellowship, while MK is supported in part by NSF grant PHY-0331516. D JW wishes to thank the University of Waterloo Physics Department for their ongoing hospitality and MK would like to thank the Perimeter Institute for Theoretical Physics for partial support and hospitality while this work was being performed.

References

- [1] J.M. Maldacena, The large N limit of superconformal field theories and supergravity, *Adv. Theor. Math. Phys.* 2 (1998) 231 [*Int. J. Theor. Phys.* 38 (1998) 1113], [hep-th/9711200](#).
- [2] E.Witten, Anti-de Sitter space, thermal phase transition, and confinement in gauge theories, *Adv. Theor. Math. Phys.* 2 (1998) 505, [hep-th/9803131](#).
- [3] C.C. Sasaki, H. Ooguri, Y. Oz and J. Terning, Glueball mass spectrum from supergravity, *J. High Energy Phys.* 01 (1999) 017, [hep-th/9806021](#); R. de Melo Koch, A. Jevicki, M. M. Ishaiescu and J.P. Nunes, Evaluation of glueball masses from supergravity, *Phys. Rev. D* 58 (1998) 105009, [hep-th/9806125](#); H. Ooguri, H. Robins and J. Tannenhauser, Glueballs and their Kaluza-Klein cousins, *Phys. Lett. B* 437 (1998) 77, [hep-th/9806171](#); J.A. Minahan, Glueball mass spectra and other issues for supergravity duals of QCD models, *J. High Energy Phys.* 01 (1999) 020, [hep-th/9811156](#); N.R. Constable and R.C. Myers, Spin-two glueballs, positive energy theorems and the AdS/CFT correspondence, *J. High Energy Phys.* 10 (1999) 037, [hep-th/9908175](#); R.C. Brower, S.D. Mathur and C. Tan, Glueball spectrum for QCD from AdS supergravity duality, *Nucl. Phys. B* 587 (2000) 249, [hep-th/0003115](#).
- [4] O. Aharony, A. Fayyazuddin and J.M. Maldacena, The large- N limit of $N = 2;1$ field theories from threebranes in F-theory, *J. High Energy Phys.* 07 (1998) 013, [hep-th/9806159](#).
- [5] A. Karch and L. Randall, Open and closed string interpretation of SUSY CFT's on branes with boundaries, *J. High Energy Phys.* 06 (2001) 063, [hep-th/0105132](#).
- [6] A. Karch and E. Katz, Adding flavor to AdS/CFT, *J. High Energy Phys.* 06 (2002) 043, [hep-th/0205236](#).
- [7] M. Karczynski, D. Mateos, R.C. Myers and D.J. Winters, Meson spectroscopy in AdS/CFT with flavor, *J. High Energy Phys.* 07 (2003) 049, [hep-th/0304032](#).
- [8] T. Sakai and J. Sonnenschein, Probing flavored mesons of confining gauge theories by supergravity, [hep-th/0305049](#).

[9] J. Babington, J. Erdmenger, N. Evans, Z. Guralnik and I. Kirsch, Chiral symmetry breaking and pions in non-supersymmetric gauge/gravity duals, hep-th/0306018.

[10] C. Nunez, A. Paredes and A. V. Ramallo, Flavoring the gravity dual of $N = 1$ Yang-Mills with probes, hep-th/0311201.

[11] N. Itzhaki, J.M. Maldacena, J. Sonnenschein and S. Yankielowicz, Supergravity and the large N limit of theories with sixteen supercharges, Phys. Rev. D 58 (1998) 046004, hep-th/9802042.

[12] O. DeWolfe, D. Z. Freedman and H. Ooguri, Holography and Effect Conformal Field Theories, Phys. Rev. D 66 (2002) 025009, hep-th/0111135.

[13] M. Gell-Mann, R. J. Oakes and B. Renner, Behavior of current divergences under $SU(3) \times SU(3)$, Phys. Rev. 175 (1968) 2195.

[14] C. Vafa and E. Witten, Restrictions on symmetry breaking in vector-like gauge theories, Nucl. Phys. B 234 (1984) 173.

[15] G. T. Horowitz and R. C. Myers, The AdS/CFT correspondence and a new positive energy conjecture for general relativity, Phys. Rev. D 59 (1999) 026005, hep-th/9808079.

[16] M. A. Shifman, A. I. Vainshtein and V. I. Zakharov, QCD and resonance physics. Sum rules., Nucl. Phys. B 147 (1979) 385.

[17] U. H. Danielsson, E. Keski-Vakkuri and M. Kruczenski, Vacua, propagators, and holographic probes in AdS/CFT, JHEP 9901 (1999) 002, hep-th/9812007.

[18] R. C. Myers, Dielectric-Branes, J. High Energy Phys. 12 (1999) 022, hep-th/9910053.

[19] R. Dijkgraaf, J.M. Maldacena, G.W. Moore and E. Verlinde, A black hole farey tail, hep-th/0005003.

[20] R. C. Myers, Stress tensors and Casimir energies in the AdS/CFT correspondence, Phys. Rev. D 60 (1999) 046002, hep-th/9903203; S. Surya, K. Schleich and D. M. Wilt, Phase transitions for large N at AdS black holes, Phys. Rev. Lett. 86 (2001) 5231, hep-th/0101134.

[21] S. J. Rey, S. Theisen and J. T. Yee, Wilson-Polyakov loop at finite temperature in large N gauge theory and anti-de Sitter supergravity, Nucl. Phys. B 527 (1998) 171, hep-th/9803135.

[22] K. Skenderis and M. Taylor, Branes in AdS and pp-wave spacetimes, J. High Energy Phys. 06 (2002) 025, hep-th/0204054.

[23] D. Mateos, S. Ng and P. K. Townsend, Supersymmetric Effect Expansion in CFT from AdS Supertubes, J. High Energy Phys. 07 (2002) 048, hep-th/0207136.

[24] J. F. Donoghue, E. Golowich and B. R. Holstein, Dynamics of the standard model, Cambridge University Press, 1992.

[25] I. R. Klebanov, P. Ouyang and E. Witten, A gravity dual of the chiral anomaly, Phys. Rev. D 65 (2002) 105007, hep-th/0202056.

[26] M. J. Strassler, Non-supersymmetric theories with light scalar fields and large hierarchies, hep-th/0309122.